T.E. NORTHUP

UNCLASSIFIED

CENTRAL RESEARCH LIBRARY
DOCUMENT COLLECTION

MARTIN MARIETTA ENERGY SYSTEMS LIBRARIES
3 4456 0350463 3

ORNL-2224, Vol. I
Physics Cy. 4

# TRANSMISSION OF OBLIQUELY INCIDENT GAMMA-RADIATION THROUGH STRATIFIED SLAB BARRIERS

C. D. Zerby

CENTRAL RESEARCH LIBRARY
DOCUMENT COLLECTION
LIBRARY LOAN COPY
Owner
DO NOT TRANSFER TO ANOTHER PERSON
If you wish someone else to see this document, send in name with document and the library will arrange a loan.

OAK RIDGE NATIONAL LABORATORY
OPERATED BY
UNION CARBIDE NUCLEAR COMPANY
A Division of Union Carbide and Carbon Corporation
UCC
POST OFFICE BOX X · OAK RIDGE, TENNESSEE

UNCLASSIFIED

Printed in USA. Price 50 cents. Available from the

Office of Technical Services
U. S. Department of Commerce
Washington 25, D. C.

LEGAL NOTICE

This report was prepared as an account of Government sponsored work. Neither the United States, nor the Commission, nor any person acting on behalf of the Commission:

A. Makes any warranty or representation, express or implied, with respect to the accuracy, completeness, or usefulness of the information contained in this report, or that the use of any information, apparatus, method, or process disclosed in this report may not infringe privately owned rights; or

B. Assumes any liabilities with respect to the use of, or for damages resulting from the use of any information, apparatus, method, or process disclosed in this report.

As used in the above, "person acting on behalf of the Commission" includes any employee or contractor of the Commission to the extent that such employee or contractor prepares, handles or distributes, or provides access to, any information pursuant to his employment or contract with the Commission.

UNCLASSIFIED

ORNL-2224, Vol. I

Applied Nuclear Physics Division

Contract No. W-7405-eng-26

# TRANSMISSION OF OBLIQUELY INCIDENT GAMMA-RADIATION THROUGH STRATIFIED SLAB BARRIERS

C. D. Zerby

Date Issued

NOV 29 1956

OAK RIDGE NATIONAL LABORATORY
Operated by
UNION CARBIDE NUCLEAR COMPANY
A Division of Union Carbide and Carbon Corporation
Post Office Box X
Oak Ridge, Tennessee

UNCLASSIFIED

MARTIN MARIETTA ENERGY SYSTEMS LIBRARIES

3 4456 0350463 3

## INTERNAL DISTRIBUTION

1. C. E. Center
2. Biology Library
3. Health Physics Library
4-5. Central Research Library
6. Reactor Experimental Engineering Library
7-26. Laboratory Records Department
27. Laboratory Records, ORNL R.C.
28. A. M. Weinberg
29. L. B. Emlet (K-25)
30. J. P. Murray (Y-12)
31. J. A. Swartout
32. E. H. Taylor
33. E. D. Shipley
34. A. H. Snell
35. M. L. Nelson
36. W. H. Jordan
37. S. J. Cromer
38. G. E. Boyd
39. R. A. Charpie
40. S. C. Lind
41. F. L. Culler
42. A. Hollaender
43. J. H. Frye, Jr.
44. M. T. Kelley
45. R. S. Livingston
46. K. Z. Morgan
47. T. A. Lincoln
48. A. S. Householder
49. C. P. Keim
50. C. S. Harrill
51. C. E. Winters
52. D. S. Billington
53. D. W. Cardwell
54. E. M. King
55. A. J. Miller
56. E. P. Blizard
57. D. D. Cowen
58. W. M. Breazeale (consultant)
59. M. J. Skinner
60. R. B. Murray
61. F. C. Maienschein
62. R. R. Dickison
63. A. Simon
64. S. Auslender
65. A. D. Callihan
66. G. T. Chapman
67. C. E. Clifford
68. A. T. Futterer
69. C. A. Goetz
70. F. L. Keller
71. H. S. Moran
72. R. W. Peelle
73. K. Penny
74-83. C. D. Zerby
84. J. A. Harvey
85. ORNL - Y-12 Technical Library, Document Reference Section

## EXTERNAL DISTRIBUTION

86. R. F. Bacher, California Institute of Technology
87. Division of Research and Development, AEC, ORO
88-684. Given Distribution as shown in TID-4500 (12th ed.) under Physics category (200 copies - OTS)

# PREFACE

This report represents the final product of an investigation of the penetration of gamma radiation through stratified slabs using a Monte Carlo method of computation. Since this method provides a bulk of information not generally available as a result of the use of other methods of computation, a considerable effort was made to make available all the data obtained without restriction because of its usefulness in many applications. The data is presented in the form of tables and graphs in Volumes I and II.

Volume I of this report contains a detailed discussion of all methods and techniques used throughout the investigation along with much of the data in the form of tables and graphs for ease of comparison of results of cases with slightly different boundary conditions.

Volume II contains the detailed angular and degraded energy spectrum of penetrating gamma radiation and the energy spectrum of the radiation reflected from many of the slabs. The total amounts of radiation reflected and penetrating each slab will be found in Volume I.

# TABLE OF CONTENTS


| CHAPTER | | PAGE |
|---|---|---|
| I. | INTRODUCTION | 1 |
| | General Introduction | 1 |
| | Summary of Solutions to the Gamma Radiation Penetration Problem | 2 |
| | Description of the Problem | 6 |
| II. | GAMMA-RAY CROSS SECTIONS | 9 |
| | Processes by which Photons Interact with Matter | 9 |
| | Cross Section Formulas | 15 |
| III. | MATHEMATICAL PROCEDURE | 21 |
| | Introduction | 21 |
| | Procedure | 21 |
| IV. | RESULTS OF CALCULATION AND DISCUSSION | 25 |
| | Presentation of Calculated Data | 25 |
| | Accuracy of the Calculation | 46 |
| | Discussion of Stratified Slab Data | 66 |
| BIBLIOGRAPHY | | 70 |
| APPENDIX A | | 73 |
| APPENDIX B | | 80 |

# LIST OF TABLES


| TABLES | | PAGE |
|---|---|---|
| I. | Photon Interaction Processes and Secondary Radiation Affecting the Transport of Gamma Rays Below 10 Mev | 10 |
| II. | Forward Scattering Cone (Deg) into Which 60 to 70 Percent of all Coherently Scattered Photons Are Directed | 13 |
| III. | Photoelectric and Pair-Production Cross Sections for Lead Calculated from Empirical Equations Compared with Those Given by White | 19 |
| IV. | Boundary Conditions Used for Solution of the Problem of Transmission of Gamma Radiation Through Slabs | 36 |
| V. | Physical Constants of Polyethylene and Lead | 37 |
| VI. | Total Photon and Energy Distribution of $Co^{60}$ Photons ($2.45\ m_oc^2$) Slant Incident on a Lead Slab | 38 |
| VII. | Total Photon Distribution Between 0.1727 and $2.45\ m_oc^2$ of $Co^{60}$ Photons ($2.45\ m_oc^2$) Slant Incident on a Polyethylene Slab | 39 |
| VIII. | Total Energy Distribution Between 0.1727 and $2.45\ m_oc^2$ of $Co^{60}$ Photons ($2.45\ m_oc^2$) Slant Incident on a Polyethylene Slab | 40 |
| IX. | Total Photon Distribution Between 0.1727 and $2\text{-}m_oc^2$ of $2\text{-}m_oc^2$ Photon Slant Incident on a Stratified Slab of Polyethylene Backed by Lead | 41 |

LIST OF TABLES (cont.)

TABLES PAGE

X. Total Energy Distribution Between 0.1727 and 2-$m_oc^2$ of 2-$m_oc^2$ Photons Slant Incident on a Stratified Slab of Polyethylene Backed by Lead . . . . . 42

XI. Total Photon Distribution Between 0.1727 and 6-$m_oc^2$ of 6-$m_oc^2$ Photons Slant Incident on a Stratified Slab of Polyethylene Backed by Lead . . . . . 43

XII. Total Energy Distribution Between 0.1727 and 6-$m_oc^2$ of 6-$m_oc^2$ Photons Slant Incident on a Stratified Slab of Polyethylene Backed by Lead . . . . . 44

XIII. Degraded Energy Spectrum of Transmitted Photons as Fraction of 2-$m_oc^2$ Photons Incident at 0 Deg on Stratified Slabs . . . . . 47

XIV. Degraded Energy Spectrum of Transmitted Photons as Fraction of 2-$m_oc^2$ Photons Incident at 30 Deg on Stratified Slabs . . . . . 48

XV. Degraded Energy Spectrum of Transmitted Photons as Fraction of 2-$m_oc^2$ Photons Incident at 60 Deg on Stratified Slabs . . . . . 49

XVI. Degraded Energy Spectrum of Transmitted Photons as Fraction of 6-$m_oc^2$ Photons Incident at 0 Deg on Stratified Slabs . . . . . 50

LIST OF TABLES (cont.)

TABLES PAGE

XVII. Degraded Energy Spectrum of Transmitted Photons as Fraction of 6-$m_oc^2$ Photons Incident at 30 Deg on Stratified Slabs . . . . . 51

XVIII. Degraded Energy Spectrum of Transmitted Photons as Fraction of 6-$m_oc^2$ Photons Incident at 60 Deg on Stratified Slabs . . . . . 52

XIX. Energy Spectrum of Photons Penetrating a Slab with Degraded Energy . . . . . 78

# LIST OF FIGURES


FIGURES PAGE

1. Slab Geometry Showing Three Typical Life Histories of the Incident Photons . . . . . 7
2. Values of $\cos\theta_{i+1}$ Associated with the Random Number $R_n$ . . . 29
3. Vector Diagram of a Typical Scattering Collision . . . . . 31
4. Flow Disgram of Calculation for Gamma-Ray Penetration of Stratified Slab . . . . . 33
5. Comparison of Calculated Values of Fraction of Energy of Gamma Radiation Incident at 0 Deg that is Transmitted Through Lead Slab . . . . . 55
6. Comparison of Calculated Values of the Fraction of Energy of Gamma Radiation Incident at 60 Deg That is Transmitted Through Lead Slabs . . . . . 56
7. Comparison of Calculated Values of the Fraction of Slant Incident Source Photons Transmitted Through Lead Slabs . . . . . 57
8. Comparison of Calculated Values of the Fraction of Energy of Gamma Radiation Incident at 0 Deg That is Transmitted Through Slabs Composed of Pure Compton Scatterer . . . . . 59
9. Comparison of Calculated and Experimental Values of the Fraction of Detector Response for the Case of $Co^{60}$ Source Photons Incident at 0 Deg on a Lead Slab . . 62

LIST OF FIGURES (cont.)

FIGURE PAGE

10. Comparison of Calculated and Experimental Values of the Fraction of Detector Response for the Case of $Co^{60}$ Source Photons Incident at 60 Deg on a Lead Slab . . . . . 63

11. Comparison of Calculated and Experimental Values of the Fraction of Detector Response for the Case of 2.00 $m_oc^2$ Photons Incident at 0 Deg on a Stratified Slab of Polyethylene Followed by 0.5 in. of Lead . . . . . 64

12. Fraction of Energy of Slant Incident 2-$m_oc^2$ Photons That is Transmitted Through Stratified Slabs of Polyethylene Backed by Lead . . . . . 67

13. Fraction of Energy of Slant Incident 6-$m_oc^2$ Photons That is Transmitted Through Stratified Slabs of Polyethylene Backed by Lead . . . . . 68

14. Energy Spectrum Resulting from Degraded Normally Incident 6-$m_oc^2$ Photons Transmitted Through Stratified Slab of 9 in. of Polyethylene Backed by Lead . . . . . 69

15. Values of $\overline{F_2(\theta')}$, $F_2(\theta')$, and $F_2(\theta')\sec\theta'$ for the Case of 2.45 $m_oc^2$ Source Photons Incident at 0 Deg on 2.5 cm of Lead . . . . . 79

LIST OF FIGURES (cont.)

FIGURE PAGE

16. Angle Variables for Source and Exit Planes of a Slab . . . . . 82

17. Plot of $G_1(\theta,E_o)$ for Stratified Slab Where 9 in. of Polyethylene is Followed by 0.3 in. of Lead and $\alpha_o = 6\text{-}m_oc^2$ . . . . . 84

18. Plot of $2uG_1(u,\alpha_o)$ for Stratified Slabs Where 9 in. of Polyethylene is Followed by 0.3 in. of Lead and $\alpha_o = 6\text{-}m_oc^2$ . . . . . 85

# CHAPTER I

# INTRODUCTION

## General Introduction

In many experiments and applications involving gamma-radiation one is confronted with the problem of estimating what fraction of the energy of a beam of gamma rays will penetrate a given thickness of material. It is also of importance in some cases to obtain a knowledge of how the incident radiation energy spectrum is modified upon passing through the barrier. These problems are especially important in the design and application of radiation shielding.

Although there have been many contributions to the theoretical treatment of the gamma-ray penetration problem in the last decade, most of the solutions have been limited to sources in an infinite or semi-infinite medium; relatively few solutions exist for barriers of a single material and of finite thickness. Solutions for finitely thick stratified barriers consisting of layers of different materials have not as yet appeared although that particular structure of a radiation barrier is quite common in application.

This report describes a method of calculation to obtain solutions to the latter problem discussed above and presents solutions to the particular problem of a stratified slab barrier consisting of a layer of polyethylene and a layer of lead.

## Summary of Solutions to the Gamma-Radiation Penetration Problem

Only a brief summary of solutions to the gamma-radiation penetration problem is included here. An extensive summary has been presented by Goldstein and Aronson.[1]

The usual approach to the problem has been to obtain approximate solutions of the Boltzmann equation[2] for a given geometry since only the simplest geometries can be considered without extreme difficulty. In most every case the simplified geometry considered has been of an infinite or semi-infinite medium. Still other simplifications regarding the behavior of the cross sections have to be made for analytic solutions to be possible. The "straight ahead" analytic solution has been obtained by altering the scattering cross section so as to consider energy degradation without deflection and, in addition, by obtaining an empirical relation for the absorption cross section over certain energy ranges in which the solution

---

[1]H. Goldstein and R. Aronson, Status Report on Calculations of Gamma Ray Penetration, (Nuclear Development Associates Report), report number NYO-3079 (1953).

[2]H. Goldstein and J. E. Wilkins, Jr., Calculations of the Penetration of Gamma Rays, (USAEC Technical Information Service Report), report number NYO-3075 (1954), p. 24.

will apply.[3-5] Other solutions presented in the literature use approximations to the Boltzmann equation which account for small angle scattering and yield asymptotic forms for the exact solution.[6-10] Numerical methods of solution of the Boltzmann equation have also been developed which use tabulated data for cross sections and are not as limited as the analytic solutions. The results of a large calculation program using a numerical method proposed by Spencer and Fano[11,12] have been given by Goldstein and Wilkins.[13]

---

[3]G. Young, Piece-Wise Greuling Solution for Hydrogen, (Oak Ridge National Laboratory Report), report number ORNL-415 (1949).

[4]G. Young, On Straight-Ahead $\gamma$-Transmission With a Minimum in the Cross Section, (Oak Ridge National Laboratory Report), report number ORNL-416 (1949).

[5]Wilkins, Oppenheim, and Solon, The Transport Equation in Straight-Ahead Case, (USAEC Report), report number NYO-633 (1950).

[6]Bethe, Fano, and Karr, Part I, Phys. Rev. 76, 538 (1949); U. Fano, Part II, Phys. Rev. 76, 739 (1949); P. R. Karr and J. C. Lankin, Part III, Phys. Rev. 76, 1843 (1949); L. V. Spencer and F. Jenkins, Part IV, Phys. Rev. 76, 1885 (1949).

[7]L. L. Foldy, Part I, Phys. Rev. 81, 395 (1951); L. L. Foldy and R. K. Osborn, Part II, Phys. Rev. 81, 400 (1951); L. L. Foldy, Part III, Phys. Rev. 82, 927 (1951).

[8]Solon, Wilkins, Oppenheim, and Goldstein, Gamma-Transmission by RMS Angle Calculation, (USAEC Technical Information Service Report), report number NYO-637 (1951).

[9]L. V. Spencer, Phys. Rev. 88, 793 (1952).

[10]L. V. Spencer, Penetration and Diffusion of X-rays by Semi-Asymptotic Methods, (National Bureau of Standards Report) report number NBS-1726 (1952).

[11]L. V. Spencer and U. Fano, Phys. Rev. 81, 464 (1951).

[12]L. V. Spencer and U. Fano, NBS Jour. Res. 46, 446 (1951).

[13]H. Goldstein and J. E. Wilkins, Jr., op. cit.

There are two methods which appear in the literature which have been used to take into account boundaries in the gamma-radiation transmission problem. Both of the methods were used to consider finitely thick slab geometry where the slab was composed of a single material. The first was the "Monte Carlo" method first suggested by von Neumann and Ulam and used by Kahn[14] on the penetration of 2.5-$m_0c^2$ photons normally incident on slabs composed of a pure Compton scatterer. Perkins[15] and Berger and Doggett[16] also used the Monte Carlo method for the penetration of slabs. The second was the "multiple scattering" method used by Peebles[17,18] to calculate the transmission through slabs of various materials.

The multiple scattering method consists of determining the transmission from those photons that have made relatively few collisions. An equation was written for the successive scattering contributions to the transmitted radiation which was then solved numerically. Because the

---

[14] H. Kahn, Nucleonics, Part I, 6, 27 (May, 1950).

[15] J. F. Perkins, J. Appl. Phys. 26, 1372 (1955).

[16] M. J. Berger and J. Doggett, Reflection and Transmission of $\gamma$-Radiation by Barriers: Semi-Analytic Monte Carlo Calculation, to be published.

[17] G. H. Peebles, Phys. Rev. 83, 237 (1951).

[18] G. H. Peebles, Gamma Ray Transmission Through Finite Slabs, (Rand Corporation Report) report number R-240 (1952).

burden of computation increases rapidly with the number of scatterings considered, only three were considered by Peebles. The calculation is thus limited to materials where the principle contribution to the transmission is from photons making a maximum of three scatterings. These results cannot be applied reliably to thick slabs consisting of light elements. It is possible to estimate the effect of the multiple scattered component for the case of a slab composed of a single material (this was done by Peebles); it is not easy to do this for the case of the stratified slab.

The Monte Carlo method is a statistical method whereby the mathematical analogue of the actual physical process is created. In practice this consists of generating the history of a relatively few photons by random sampling techniques and estimating the result for a large number of photons. If the mathematical expressions for scattering, energy degradation, absorption, etc. are correct, then the process corresponds to estimating the results of a high intensity experiment from the results of a low intensity experiment. The amount of information that can be obtained from such a calculation is limited only by the variance of the various estimates. In principle, geometry and source distribution form no obstacle to the calculation; in practice, however, they are limited by sampling requirements of the photon phase space (energy, scattering angle, and space coordinates) with a reasonable number of photon histories. Insufficient sampling of the phase space could result in a gross underestimate of the answer sought without indication from the calculated variance that anything was wrong. A typical example of this is the calculation of the penetration

of very thick slabs where the deep lying layers of the slab are sampled inadequately because of the large attenuation factor. A general discussion of this point and of the Monte Carlo method in general is given by Kahn.[19]

## Description of the Problem

The geometry selected for investigation was a finitely thick slab of infinite extent with plane parallel faces where the source was a monochromatic, monodirectional plane wave of gamma-radiation incident over one face of the slab. With this particular set of conditions the calculation was directly comparable to the experiment of Kirn, Kennedy, and Wyckoff.[20]

A parameter study was made of lead slabs and polyethylene slabs using the above described geometry where the radiation was incident at several different angles of incidence but was considered to come from Cobalt-60 source. A parameter study was also made of a stratified slab consisting of a layer of polyethylene followed by a layer of lead as shown in Fig. 1. However, in the latter case two different source energies were taken at two and six electron rest mass units of energy. It should be pointed out that the use of the source selected does not restrict the

---

[19] H. Kahn, op. cit.

[20] F. S. Kirn, R. J. Kennedy, and H. O. Wyckoff, Radiology, 63, 94 (July, 1954).

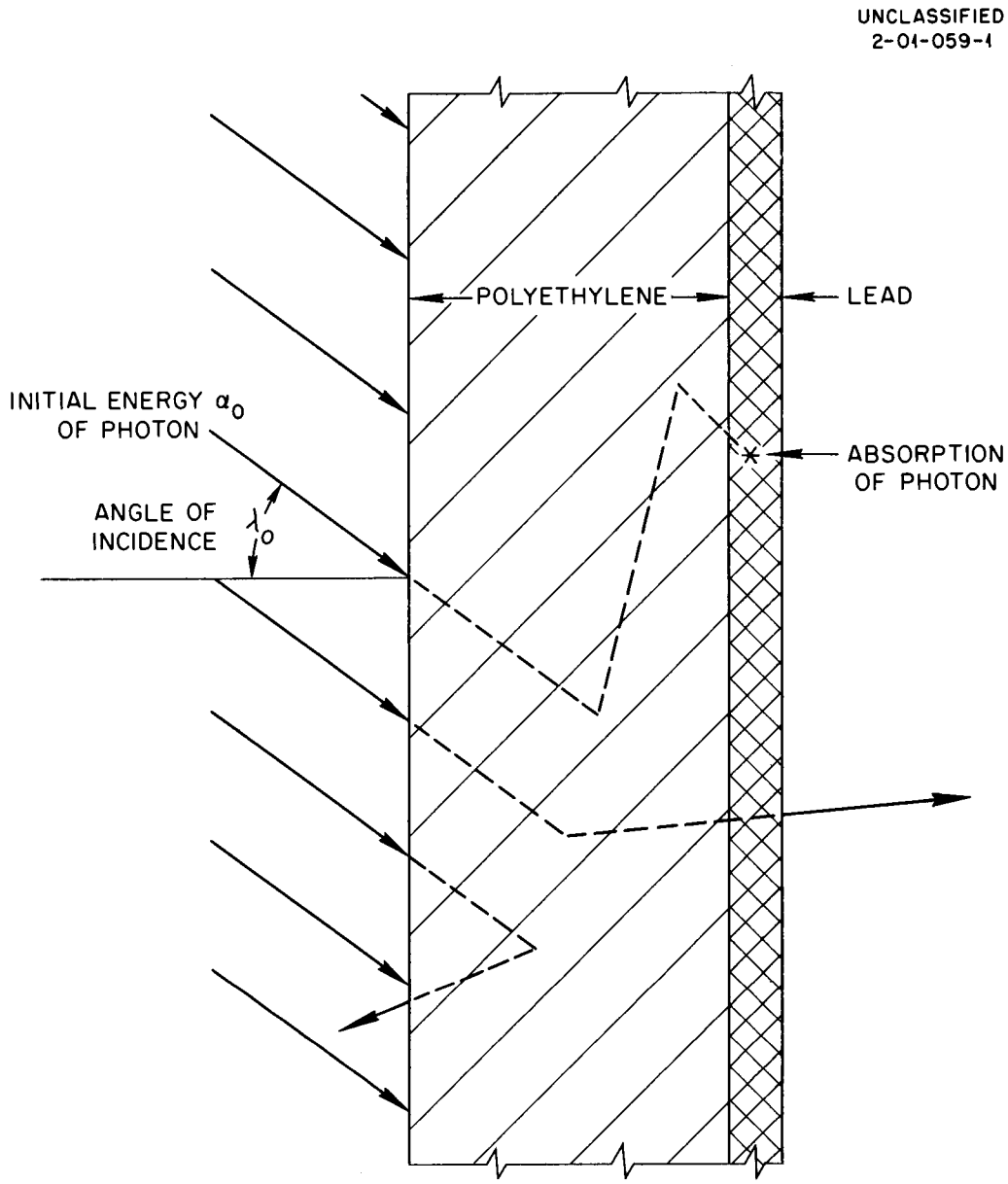


Fig. 1. Slab Geometry Showing Three Typical Life Histories of the Incident Photons.

general nature of the problem since it is possible to construct the transmission for any complex source spectra and angular distribution from the results of the monodirectional, monochromatic beams as shown in Appendix B.

In Chapter II a detailed discussion is given of the processes by which gamma rays interact with matter. In most cases the interactions are of little importance and can be ignored in a problem of this type; however, pair-production, photoelectric effect, and Compton scattering cannot be ignored and were considered in this study. The photoelectric effect and pair-production were assumed to be pure absorptions in which the total energy of the photon is transferred to the material. Compton scattering of the photons was assumed to be the only process by which the photon could give up energy to the medium without being absorbed.

All the conditions set on the problem were such that the Monte Carlo method of calculation was the only one that offered a means of computation without serious limitations. For this reason that method was used and the problem was programmed and coded for calculation on the ORACLE, the high speed electronic computor located at the Oak Ridge National Laboratory.

# CHAPTER II

## GAMMA RAY CROSS SECTIONS

### Processes by Which Photons Interact with Matter

The processes by which photons interact with matter are well known. A detailed description of them has been given by many authors.[21-24] In the following only enough of a description of the individual processes will be included to justify the cross sections selected for the calculation.

Table I includes a list of processes which affect the transport, and thus the transmitted energy spectrum, of gamma rays through matter in the energy region below 10 Mev. The absorption processes listed are those in which the interacting photon disappears losing all of its energy; the scattering processes are the various ones which will cause the interacting photon to be deflected in its path and, in most cases, with some loss in energy. The list of secondary radiation resulting from a photon

---

[21] W. Heitler, The Quantum Theory of Radiation, (Oxford Press, 1954).

[22] H. A. Bethe and J. Ashkin, "Penetration of Gamma Rays," Vol. 1, Part II-3 of Experimental Nuclear Physics, E. Segre, Ed., (John Wiley and Sons, Inc., New York, 1953).

[23] U. Fano, Part I, Nucleonics 11, 8 (Aug. 1953); Part II Nucleonics 11, 35 (Sept. 1953); and "Gamma Ray Attenuation," Vol. 1, Chap. 2.3, Reactor Handbook (USAEC Technical Information Service report), report number AECD-3645 (1955).

[24] G. R. White, X-Ray Attenuation Coefficients from 10 kev to 100 Mev, (National Bureau of Standards Report), report number NBS-1003 (1952).

TABLE I

PHOTON INTERACTION PROCESSES AND SECONDARY RADIATION AFFECTING THE TRANSPORT OF GAMMA RAYS BELOW 10 MEV

Absorption processes

1. Electron photoelectric effect
2. Atomic pair-production
3. Nuclear photoelectric effect

Scattering processes

1. Incoherent (Compton)
2. Coherent (Rayleigh)
3. Nuclear (Resonance)
4. Nuclear (Thompson)
5. Potential (Delbruck)

Secondary radiation

1. Bremsstrahlung
2. Annihilation
3. Fluorescence

absorption or scattering includes only those that can contribute to the transmitted gamma-ray energy spectrum.

In this calculation only the electron photoelectric effect (hereafter simply called photoelectric effect), atomic pair-production, and Compton scattering were taken into consideration. The first two were treated as pure absorption effects. Of the other processes given in Table I it is easy to justify neglecting nuclear photoelectric effect, nuclear resonance and Thompson scattering, and Delbruck scattering because of their insignificant cross sections compared to the three processes retained in the calculation.[25] These processes could not affect the over-all penetration problem to a degree that would warrant the additional complication caused by their inclusion; their total effect should be well within the limits of accuracy of the calculation. The other neglected processes cannot be ignored with so simple an explanation but have to be treated individually.

Coherent, or Rayleigh, scattering of photons from the electron cloud of an atom involves no loss of photon energy and the scattered gamma rays interfere constructively in a predominantly forward direction which is dependent on the atomic number Z and the gamma ray energy $\alpha$. The differential cross section per electron for this process is given by[26]

---

[25] H. A. Bethe and J. Ashkin, op. cit., p. 345-349.

[26] A. H. Compton and S. K. Allison, X-Rays in Theory and Experiment, (D. Van Nostrand Company, Inc., New York, 1935), p. 140.

$$d\sigma = \frac{r_e^2(1 + \cos^2\theta)}{2Z} \left[F(\alpha,\theta,Z)\right]^2 d\Omega \qquad (1)$$

where

$\theta$ = angle of scattering,

$r_e$ = classical electron radius,

$\Omega$ = solid angle,

$F(\alpha,\theta,Z)$ = atomic form factor.

The function $F(\alpha,\theta,Z)$ has been tabulated in part by Compton and Allison.[27] In general, the atomic form factor decreases with increasing $\alpha$ and $\theta$ but increases with increasing Z. The dependence of the differential cross section on these variables can be observed from the data presented in Table II which was taken from Fano.[28] In Table II the angles quoted for the forward scattering are chosen such that an estimated 60 to 70 percent of the photons are directed into the cone when coherently scattered.

Although the coherent scattering cross section increases rapidly with Z it still remains small compared to the total cross section since the photoelectric effect also increases rapidly with Z. For 0.1 Mev photons the coherent cross section for lead is only 3% of the total cross section[29] which is typical for all materials at a photon energy of 0.1 Mev.

---

[27] A. H. Compton and S. K. Allison, Ibid, Appendix IV.

[28] U. Fano, Nucleonics 11, 8 (Aug. 1953), p. 11.

[29] G. R. White, op. cit., p. 19.

TABLE II

FORWARD SCATTERING CONE (DEG) INTO WHICH 60 TO 70 PERCENT OF ALL COHERENTLY SCATTERED PHOTONS ARE DIRECTED

| Energy (Mev) | 0.1 | 1 | 10 |
|---|---|---|---|
| Al (Z = 13) | 15 | 2 | 0.5 |
| Fe (Z = 26) | 20 | 3 | 0.8 |
| Pb (Z = 82) | 30 | 4 | 1.0 |

In order to avoid undue complication to the problem it seemed reasonable to neglect the coherent scattering completely. Reducing the total cross section by the amount of the coherent scattering cross section makes a small percentage change; however, it actually introduces the approximation that the coherent scattered photons are directed straight ahead rather than having an angular distribution. This approximation is very good at high energy for all materials and for much of the energy range of this problem (0.1727-6.0 $m_oc^2$) for the light elements. Since energy degradation is not involved, it is expected that the approximation will introduce an error in the angular distribution of penetrating photons but little error in the energy spectrum.

Bremsstrahlung radiation can result from collisions of electrons or positrons with atomic nuclei or electrons. The electrons and positrons created in the pair-production process or electrons ejected from the atom by the photoelectric effect and Compton recoils are, therefore, sources for this secondary radiation; however, only a small percentage of the slowing down collisions of these particles will be radiative in the energy range considered in the problem and little of the initial energy will appear as electromagnetic radiation.[30] The spectrum of the Bremsstrahlung radiation[31] also shows a predominance of low energy photons relative to the incident energy of the electron (or positron) so it is expected that the secondary radiation that is produced as Bremsstrahlung will be

---

[30] W. Heitler, op. cit., p. 252.

[31] W. Heitler, op. cit., p. 250.

quickly absorbed. The contribution to the transmission spectrum by the Bremsstrahlung radiation should be a small effect in this problem and should be concentrated in the low energy end of the spectrum. For these reasons it was neglected in the calculation, although no quantitative data has appeared to substantiate this line of reasoning.

Fluorescence and annihilation radiation have been neglected because of their relatively small effect on the penetration problem. Goldstein[32] has shown the contribution to the total penetration by fluorescence radiation to be significant only for the heaviest elements and for gamma-ray sources of less than 1 Mev primary energy. He also calculated the contribution to the total penetration by annihilation radiation and found to be significant only for high energy sources. It will not be significant for low energy sources, such as used in this problem.

## Cross Section Formulas

The angular dependence of the incoherent or Compton scattering was determined from the Klein-Nishina equation[33]

$$d\sigma^{c} = \frac{r_e^2}{2} \left(\frac{\alpha_{i+1}}{\alpha_i}\right)^2 \left(\frac{\alpha_i}{\alpha_{i+1}} + \frac{\alpha_{i+1}}{\alpha_i} - \sin^2\theta\right) d\Omega \qquad (2)$$

---

[32] H. Goldstein, Estimates of the Effect of Fluorescence and Annihilation Radiation on Gamma Ray Penetration, (Nuclear Development Associates Report), report number NDA 15C-31 (1954).

[33] W. Heitler, op. cit., p. 39.

where

$\alpha_i$ = energy of the photon before collision ($m_o c^2$),

$\alpha_{i+1}$ = energy of the photon after collision ($m_o c^2$),

$d\sigma^c$ = incoherent scattering differential cross section ($cm^2$/electron).

The relation between $\alpha_i$ and $\alpha_{i+1}$ is given by[34]

$$\alpha_{i+1} = \frac{\alpha_i}{1 + \alpha_i(1 - \cos\theta)} \quad . \tag{3}$$

The Klein-Nishina equation gives the differential cross section per free electron for incident unpolarized gamma rays and is only an approximation to the equation for incoherent scattering from an atomic electron given by

$$d\sigma = \frac{d\sigma^c}{d} \left\{ 1 - \frac{\sum_{n=1}^{Z} \left[ f_n(\alpha,\theta,Z) \right]^2}{Z} \right\} d\Omega \tag{4}$$

where

$d\sigma$ = differential cross section ($cm^2$/atomic electron),

$f_n(\alpha,\theta,Z)$ = the electronic structure factor for the $n^{th}$ electron.

The term $\sum_{n=1}^{Z} f_n(\alpha,\theta,Z)^2$ has been tabulated in part by Compton and Allison.[35] The correction term (in the curly brackets) has the effect of reducing the incoherent scattering in the forward direction from that

---

[34] W. Heitler, op. cit., p. 211, Eq. 4.

[35] A. H. Compton and S. K. Allison, loc. cit.

given by the Klein-Nishina equation. This correction becomes negligible for all elements at high energy and is of little significance for the lightest elements for energies higher than 0.01 Mev. At still lower energies the incoherent scattering cross section decreases and the angular distribution of scattering changes markedly from that given by (2); however, in the energy range of this problem these differences will be small, at least for the light elements considered, and will be small in lead for energies above 0.5 Mev. It should be noted that the increase in scattering in the forward direction indicated by (2) is not accompanied by large changes in photon energy so that the error is principally in the angular distribution of the penetrating photons rather than in the energy spectrum.

If the incident radiation were polarized, the differential cross section formula would be different from that given by (2); however, calculations by Spencer and Wolff[36] show that there is no need to introduce this additional complication.

Integration of (2) over all solid angles gives the Compton cross section

$$\sigma^c = \frac{\pi r_e^2}{\alpha_i^3(1 + 2\alpha_i)^2} \Big[ 4(1 + \alpha_i)^2(1 + 2\alpha_i)\,\alpha_i + (1 + 2\alpha_i)^2 \times (\alpha_i^2 - 2\alpha_i - 2)\,\mathrm{Ln}(1 + 2\alpha_i) - 2\alpha_i^3(1 + 3\alpha_i) \Big] \tag{5}$$

---

[36] L. V. Spencer and C. Wolff, Phys. Rev. 90, 510 (1955).

where $\sigma^c$ is the Compton cross section ($cm^2$/electron). Equation (5) was used to calculate the value of $\sigma^c$ whenever the cross section was needed in the problem.

The photoelectric and pair-production cross sections for lead were taken from the table prepared by White.[37] Empirical equations for use on the ORACLE were obtained by fitting this data over the energy range of the problem. White's data for the photoelectric effect included the cross sections for the K, L, and M shells, and the data for pair production included the cross sections in the field of the nucleus and the atomic electrons. In both cases, that data represents the best fit to theory and experiment. The empirical relation used for the photoelectric cross section was

$$\mathrm{Ln}(10^{24}\sigma^{Ph}) = -1.1893 - 2.32499a + 0.30705a^2 + 0.044107a^3 - 0.01899a^4 \quad (6)$$

where

$$a = \mathrm{Ln}\alpha_1 \qquad (0.1727 \leq \alpha_1 \leq 6),$$

$\sigma^{Ph}$ = photoelectric cross section for lead ($cm^2$/electron).

The pair-production cross sections were obtained from

$$82 \times 10^{24}\sigma^P = -0.44884 - 0.13006\alpha_1 + 0.19140\alpha_1^2 - 0.0006174\alpha_1^3 - 0.000449\alpha_1^4 \qquad (2 < \alpha_1 \leq 6) \quad (7)$$

$$= 0 \qquad (\alpha_1 \leq 2)$$

where $\sigma^P$ is the pair-production cross section for lead ($cm^2$/electron). Table III gives the values of the cross sections calculated using (6) and

---

[37] G. R. White, op. cit., Table I.

TABLE III

PHOTOELECTRIC AND PAIR-PRODUCTION CROSS SECTIONS FOR LEAD CALCULATED FROM EMPIRICAL EQUATIONS COMPARED WITH THOSE GIVEN BY WHITE[a]

| Energy $m_oc^2$ | Photoelectric Cross Section $cm^2$/electron | | Percent Difference | Pair-Production Cross Section $cm^2$/electron | | Percent Difference |
|---|---|---|---|---|---|---|
| | From Eq. (6) | White's Data | | From Eq. (7) | White's Data | |
| 0.1727 | 30.67 | 30.61 | 0.2 | | | |
| 0.2 | 20.80 | 20.80 | 0.0 | | | |
| 0.3 | 6.91 | 6.87 | 0.6 | | | |
| 0.4 | 3.17 | 3.19 | 0.6 | | | |
| 0.5 | 1.74 | 1.76 | 1.1 | | | |
| 0.6 | 1.074 | 1.075 | 0.1 | | | |
| 0.7 | 0.723 | 0.736 | 1.8 | | | |
| 0.8 | 0.519 | 0.529 | 1.9 | | | |
| 0.9 | 0.390 | 0.393 | 0.8 | | | |
| 1.0 | 0.304 | 0.302 | 0.7 | | | |
| 1.2 | 0.200 | 0.200 | 0.0 | | | |
| 1.4 | 0.144 | 0.146 | 1.4 | | | |
| 1.6 | 0.110 | 0.112 | 1.8 | | | |
| 1.8 | 0.0869 | 0.0897 | 3.1 | | | |
| 2.0 | 0.0711 | 0.0734 | 3.1 | 0 | 0 | 0 |
| 2.5 | 0.0478 | 0.0489 | 2.2 | 0.0037 | 0.0036 | 2.7 |
| 3.0 | 0.0350 | 0.0360 | 2.8 | 0.0083 | 0.0082 | 1.2 |
| 3.5 | 0.0279 | 0.0288 | 3.1 | 0.0135 | 0.0133 | 1.5 |
| 4.0 | 0.0229 | 0.0237 | 3.3 | 0.0193 | 0.0192 | 0.5 |
| 5.0 | 0.0169 | 0.0170 | 0.6 | 0.0321 | 0.0323 | 0.6 |
| 6.0 | 0.0134 | 0.0129 | 3.8 | 0.0457 | 0.0453 | 0.8 |

a. See footnote 37 in paper.

(7) as compared with extrapolated values from the data given by White. The percent errors indicated are for the differences between the empirically calculated cross sections and the values given by White. In every case the error introduced by the fit to the data will be less than 1 per cent of the total cross section.

Let us now consider the situation for polyethylene, $(CH_2)_n$. The carbon has a small pair production and photoelectric cross section in the energy range of the problem. The hydrogen has a negligible absorption cross section over the complete range, and in the energy range 0.294 to $2.0\text{-}m_0c^2$ the absorption cross section is also negligible in carbon. The photoelectric cross section rises to 1.0 per cent of the total cross section of carbon at the lowest energy considered in the problem, and the pair-production cross section rises to 2.6 per cent of the total carbon cross section at the high energy end of the range. The percentage of the total polyethylene cross section attributed to these absorption processes would be, of course, much smaller. For these reasons polyethylene was assumed to be a pure Compton scatterer throughout the problem.

# CHAPTER III

# MATHEMATICAL PROCEDURE

## Introduction

The purpose of this chapter is to describe the mathematical procedure developed for solving the problem on the ORACLE. The main body of the chapter deals with the Monte Carlo method.

Two physical assumptions were introduced for mathematical simplicity; the first was that the source strength was independent of time, and the second was that radiation leaving the slab was lost and did not return to the slab.

## Procedure

To generate a photon history, that is, to pick values of all variables describing the physical behavior of the photon from birth to death, it is, in general, necessary to determine a set of numbers $(\alpha_i, \beta_i, \theta_i, \phi_i)$, i = 0, 1, 2, 3, ....., n, where the parameters have the following physical assiciation with the history: $\alpha_i$ is the energy of the photon after the $i^{th}$ collision, $\beta_i$ is the distance traveled between the $i^{th}$ and i + 1 collision, $\theta_i$ is the angle between the direction before and after the $i^{th}$ collision, and $\phi_i$ is the azimuthal angle with respect to the direction before collision that the photon scatters after the $i^{th}$ collision. The sequence of numbers terminates at i = n when the photon is absorbed or leaves the region of interest. Each of the parameters is associated with a probability distribution from which a value

is selected by appropriate sampling techniques. The selected numbers are treated as precise values and no account is taken of the uncertainty in the values.

The numerical quantities given the variable in the probability process are called random variables. The random variable will be designated by a subscript such that $x_i$ will be a random variable associated with the variable x. The probability that any random variable $x_i$ will assume values less than or equal to x is given by the cumulative distribution function (c.d.f.) designated by a capital letter such as F(x). In the region where the function F(x) has a derivative f(x) the random variable is said to have a probability density, and f(x) is called the probability density function (p.d.f.). The probability that a random variable lies in the region between x and $x + \Delta x$ is $F(x + \Delta x) - F(x)$, or $f(x)\Delta x$ when $\Delta x$ is small. The relation between f(x) and F(x) is

$$F(x) = \int_{-\infty}^{x} f(x')dx' \tag{8}$$

Since F(x) obtains the maximum value one, in all cases f(x) should be properly normalized so that

$$\int_{-\infty}^{+\infty} f(x)dx = 1 \tag{9}$$

The above equation does not imply that f(x) has a value different from zero for every value of x in the interval $(-\infty, \infty)$ since f(x) can be defined as zero over certain ranges of the variable.

It is usually difficult to devise a random sampling technique for picking values of the random variable from the probability density functions that arise in practice so it is often necessary to transform to a p.d.f. that is easy to sample from by use of a monotonic transformation

$$R = k(x) \tag{10}$$

so that

$$f(x)dx = g(R)dR \tag{11}$$

where $g(R)$ is the new p.d.f. It is easy to see that (11) holds since there is a one to one correspondence between the variables x and R, and, as before, $f(x)dx$ is the probability $x_i$ will have a value such that $x < x_i \leq x + dx$ while $g(R)dR$ is the probability $R_i$ will have a value such that $R < R_i \leq R + dR$. By the same reasoning it follows that

$$F(x) = G(R) \tag{12}$$

or

$$F(x_i) = G(R_i) \tag{13}$$

If a random variable $R_i$ has been picked from the p.d.f. $g(R)$ it can be substituted into (13) and the equation solved for $x_i$.

Methods for obtaining pseudo random numbers uniformly distributed on the interval (0, 1) have been devised for automatic computing machines and will be discussed below. This amounts to picking from the p.d.f.

$$\begin{aligned} g(R) &= 0 & R &< 0 \\ g(R) &= 1 & 0 \leq R &\leq 1 \\ g(R) &= 0 & 1 &< R \end{aligned} \tag{14}$$

Substituting (14) into (8) where $f(x')$ is replaced with $g(R')$ it is found that

$$G(R) = R, \tag{15}$$

therefore, (13) becomes

$$\int_{-\infty}^{x_i} f(x)dx = R_i \tag{16}$$

where the relation given in (8) was used for $F(x)$. It should be noted that (10) compares with (16) and the left hand side of (16) defines $k(x_i)$.

The congruence method for generating pseudo-random numbers uniformly on an interval has been reviewed by Taussky and Todd.[38] On the ORACLE the following mathematical form was used:

$$R_{i+1} = R \cdot R_i \left[\text{Mod } 2^{39}\right] \quad i = 0, 1, 2, \ldots\ldots \tag{17}$$

where

$R = 5^{15}$,

$R_0 = 1$,

$R_j$ = a number in the sequence of random numbers.

For convenience (17) was written with all values scaled up by the factor $2^{39}$, that is, as written the values of $R_j$ are uniformly distributed over the interval $(0, 2^{39})$. In what follows, the assumption will be made that the scaling factor is removed and the values of $R_j$ are uniformly distributed over the interval (0, 1). This method of generating a sequence of random numbers is very useful having a period of $2^{37}$. In practice the numbers are generated as needed in the problem.

---

[38] O. Taussky and J. Todd, Generating and Testing of Pseudo-Random Numbers, (National Bureau of Standards Report), report number NBS-3370 (1954).

The form of f(x) used in (16) depends on the probability process. In what follows the p.d.f. for each process for generating a photon history in a slab of material will be determined.

The one dimensional character of the slab problem can be taken advantage of in several ways. The first advantage is taken in determining the normal distance traveled through the slab between collisions rather than the actual path length. The normal to the slab is assumed to have a positive direction through the slab away from the source face. The probability a photon leaving the point of the $i^{th}$ collision at an angle $\lambda_i$ with respect to the normal makes a collision in the distance dp after having traveled a distance p along the normal is

$$\frac{\sigma_i^T N}{\cos\lambda_i} e^{-\frac{\sigma_i^T N p}{\cos\lambda_i}} dp \tag{18}$$

where N is the electron density of the matter being traversed (electrons/$cm^3$) and

$$\sigma_i^T = \sigma_i^c + \sigma_i^{Ph} + \sigma_i^p \tag{19}$$

The notation $\sigma_i$ means the cross section evaluated at the energy of the photon after the $i^{th}$ collision. If the matter is lead, $\sigma_i^c$ is obtained from (5), $\sigma_i^{Ph}$ from (6), and $\sigma_i^p$ from (7). If the matter is polyethylene, the values of $\sigma_i^{Ph}$ and $\sigma_i^p$ are taken as zero, however, $\sigma_i^c$ is still obtained from (5). The p.d.f. for the distance p is obtained from (18) and is already properly normalized. Thus the p.d.f. for the distance p is

$$\begin{aligned} h(p) &= 0 & p < 0 \\ h(p) &= \frac{\sigma_i^T N}{\cos\lambda_i} e^{-\frac{\sigma_i^T N p}{\cos\lambda_i}} & p \geq 0 \end{aligned} \tag{20}$$

Substituting (20) for the p.d.f. in (16) gives

$$\int_{o}^{p_i} \frac{\sigma_i^T N}{\cos\lambda_i} e^{-\frac{\sigma_i^T N p}{\cos\lambda_i}} = R_s \tag{21}$$

where $p_i$ is the distance traveled along the normal between the $i^{th}$ and $i + 1$ collision. Solving (21) for $p_i$ gives

$$p_i = -\frac{\cos\lambda_i}{\sigma_i^T N} \operatorname{Ln}(1 - R_s), \tag{22}$$

but the numbers $1 - R_s$ are random and uniformly distributed over the interval (0, 1), therefore, (22) can be reduced to

$$p_i = -\frac{\cos\lambda_i}{\sigma_i^T N} \operatorname{Ln} R_s \tag{23}$$

The value of $p_i$ is greater or less than zero depending on the sign of $\cos\lambda_i$.

The probability that the photon survives the $i + 1$ collision is given by $\frac{\sigma_i^c}{\sigma_i^T}$. The probability that a random number $R_m \leq \frac{\sigma_i^c}{\sigma_i^T}$ is $\frac{\sigma_i^c}{\sigma_i^T}$, therefore the following test is made:

if $R_m \leq \frac{\sigma_i^c}{\sigma_i^T}$ the photon has a scattering collision otherwise it is absorbed. (24)

Assuming the photon has made a scattering collision, the angle at which it scatters was determined using the Klein-Nishina Eq. (2). Since the differential cross section equation is independent of the azimuthal angle $\phi$, the equation is integrated over the range of that variable to obtain

$$d\sigma_i^c = \pi r_e^2 \left(\frac{\alpha_{i+1}}{\alpha_i}\right)^2 \left(\frac{\alpha_i}{\alpha_{i+1}} + \frac{\alpha_{i+1}}{\alpha_i} - \sin^2\theta\right) \sin\theta d\theta. \tag{25}$$

The properly normalized p.d.f. for the variable $\theta$ is then

$$\begin{aligned} m(\theta) &= 0 && \theta < 0 \\ m(\theta) &= \frac{\pi r_e^2}{\sigma_i^c}\left(\frac{\alpha_{i+1}}{\alpha_i}\right)^2 \left(\frac{\alpha_i}{\alpha_{i+1}} + \frac{\alpha_{i+1}}{\alpha_i} - \sin\theta\right) \sin\theta && 0 \leq \theta \leq \frac{\pi}{2} \\ m(\theta) &= 0 && \frac{\pi}{2} < \theta \end{aligned} \tag{26}$$

where $\sigma_i^c$ is obtained from (5). Substituting this p.d.f. in (16) results in the following equation which must be solved for $\theta_{i+1}$:

$$\int_0^{\theta_{i+1}} m(\theta)d\theta = R_n \tag{27}$$

The unknown $\alpha_{i+1}$ is removed from $m(\theta)$ using the Compton Eq. (3), and the integration performed in (27) to obtain

$$R_n = \frac{\pi r_e^2}{2\sigma_i^c \alpha_i^3 Q^3}\Big[ - Q\alpha_i^2 - 2Q^2(1 + 2\alpha_i) + 2Q^3(\alpha_i^2 - 2\alpha_i - 2) \times \mathrm{Ln}(Q) + 2Q^4 + (\alpha_i + 4)\alpha_i Q^3\Big] \tag{28}$$

where

$$Q = 1 + \alpha_i(1 - \cos\theta_{i+1}). \tag{29}$$

The transcendental equation (28) can be solved for Q by use of the second

order Newton iteration method.[39] The iteration is defined by the equation

$$Q_{j+1} = Q_j - \frac{n(Q_j)}{n'(Q_j)} \tag{30}$$

where

$$n(Q_j) = R_n - \frac{\pi r_e^2}{2\sigma_i^c \alpha_i^3 Q_j^3} \Big[ - Q_j \alpha_i^2 - 2Q_j^2(1 + 2\alpha_i) + 2Q_j^3(\alpha_i^2 - 2\alpha_i - 2)$$

$$\times \operatorname{Ln}(Q_j) + 2Q_j^4 + (\alpha_i + 4)\alpha_i Q_j^3 \Big] \tag{31}$$

and $n'(Q_j)$ is the first derivative of $n(Q_j)$ with respect to $Q_j$ given by

$$n'(Q_j) = - \frac{\pi r_e^2}{\sigma_i^c \alpha_i^3 Q_j^3} \Big[ \alpha_i^2 + Q_j(1 + 2\alpha_i) + Q_j^2(\alpha_i^2 - 2\alpha_i - 2) + Q_j^3 \Big]. \tag{32}$$

A graph of (28) is given in Fig. 2 along the rough approximating equation

$$R_n = \left( \frac{1 - \cos\theta_{i+1}}{2} \right)^{1/2} . \tag{33}$$

Solving (33) for $\cos\theta_{i+1}$ and substituting it into (29) gives a "first guess" value for $Q_o$ which is given by

$$Q_o = 1 + 2\alpha_i R_n^2. \tag{34}$$

This simple equation gives a reasonable approximation for Q with a minimum of computation and reduces the number of iterations required considerably.

---

[39] A. S. Householder, Principles of Numerical Analysis, (McGraw-Hill Book Company, New York, 1953), p. 122.

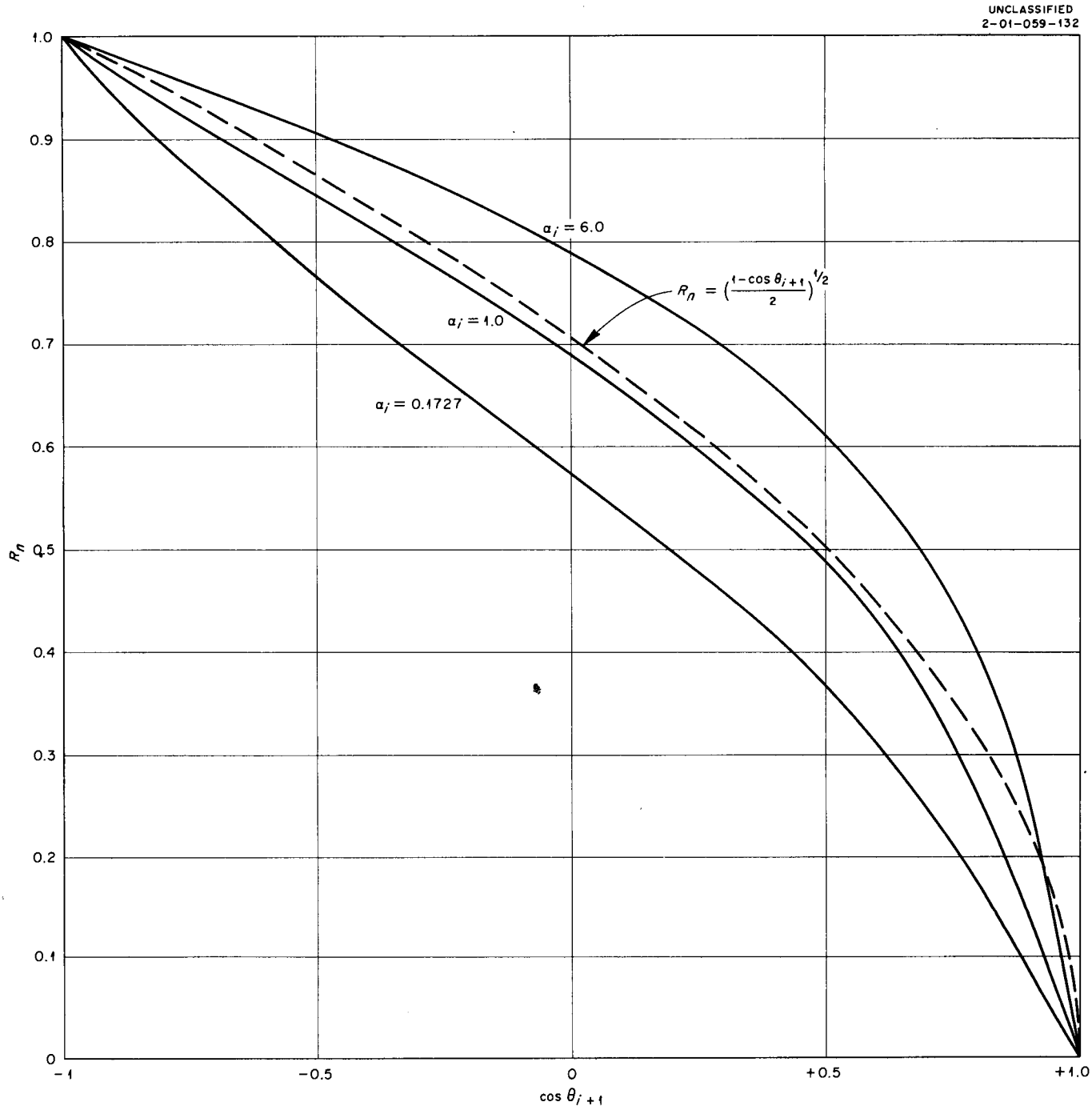


Fig. 2. Values of $\cos\theta_{i+1}$ Associated with the Random Number $R_n$ .

This avoids the use of higher order iterations and the resulting increase in computation required per iteration. The convergence criterion for the iteration was chosen as

$$\left| Q_{j+1} - Q_j \right| \leq 2^{-10} \tag{35}$$

and was achieved on the average on the third iteration.

With the random value of Q selected, the energy after collision is readily obtained from the equation

$$\alpha_{i+1} = \frac{\alpha_i}{Q} \tag{36}$$

which corresponds to Eq. (3). Equation (29) was then solved for $\cos\theta_{i+1}$ which was used rather than the value of the angle itself.

The azimuthal angle of scattering $\phi_{i+1}$ is uniformly distributed on the interval $(0, 2\pi)$, therefore, the relation between $\phi_{i+1}$ and the random number $R_p$ is simply

$$\phi_{i+1} = 2\pi R_p. \tag{37}$$

Figure 3 gives a vector diagram of a typical scattering collision showing the unit vector $\hat{n}$ along the slab normal and the unit vectors $\hat{k}_i$ and $\hat{k}_{i+1}$ along the directions before and after scattering respectively. The angle $\lambda_{i+1}$ shown in the diagram was obtained using the spherical cosine law.

$$\cos\lambda_{i+1} = \cos\lambda_i \cos\theta_{i+1} + \sin\lambda_i \sin\theta_{i+1} \cos\phi_{i+1} \tag{38}$$

UNCLASSIFIED
2-01-059-133

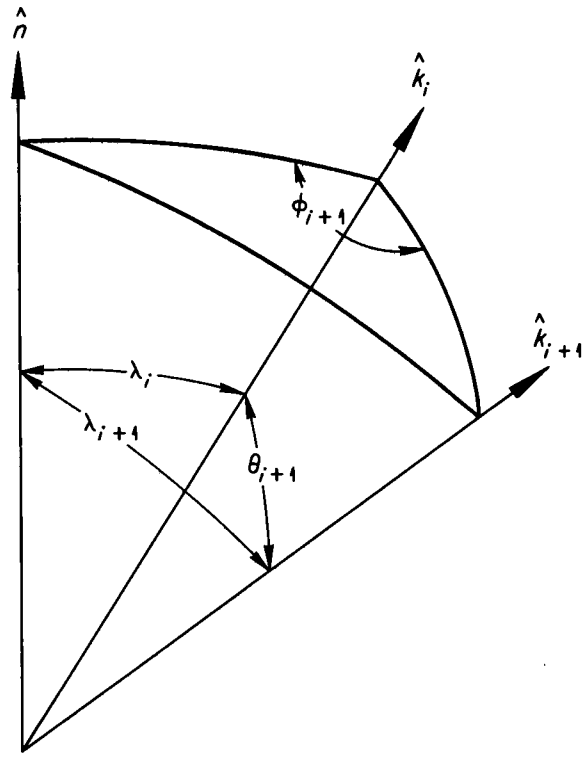


Fig. 3. Vector Diagram
of a Typical Scattering Collision.

At this point a description has been given of all random processes involved in generating a random history of a photon. The procedure incorporating these processes and followed in the calculation for the penetration of the stratified slab is shown in the "flow diagram" given in Fig. 4. In the diagram the following definitions apply:

$X$ = thickness of polyethylene,

$Y$ = thickness of lead,

$x_i$ = distance traveled along the normal in the polyethylene slab between the $i^{th}$ and $i + 1$ collision,

$y_i$ = distance traveled along the normal in the lead slab between the $i^{th}$ and $i + 1$ collision,

$M$ = number of sample photons,

$\lambda_o$ = incident angle of source photons,

$\alpha_o$ = incident energy of source photons,

$\alpha_k$ = energy of the K-edge of lead $(0.1727\text{-}m_oc^2)$.

Several aspects of the flow diagram are worthy of some discussion. The diagram has two major cycles used for the alternate cases when the photon was in polyethylene or in lead. In blocks 15 and 34 the difference between the energy before and after a scattering collision, $P_i$, was calculated and totaled $(P_T)$ for all such collisions in the respective materials. Another contribution to the energy deposited in the lead was calculated in block 30 where the entire photon energy was transferred to the lead in an absorption collision. If the photon was degraded below the energy $\alpha_k$ in either of the materials (blocks 14 and 34) the entire photon energy before collision was accumulated as energy deposited in the respective slabs. A record was also

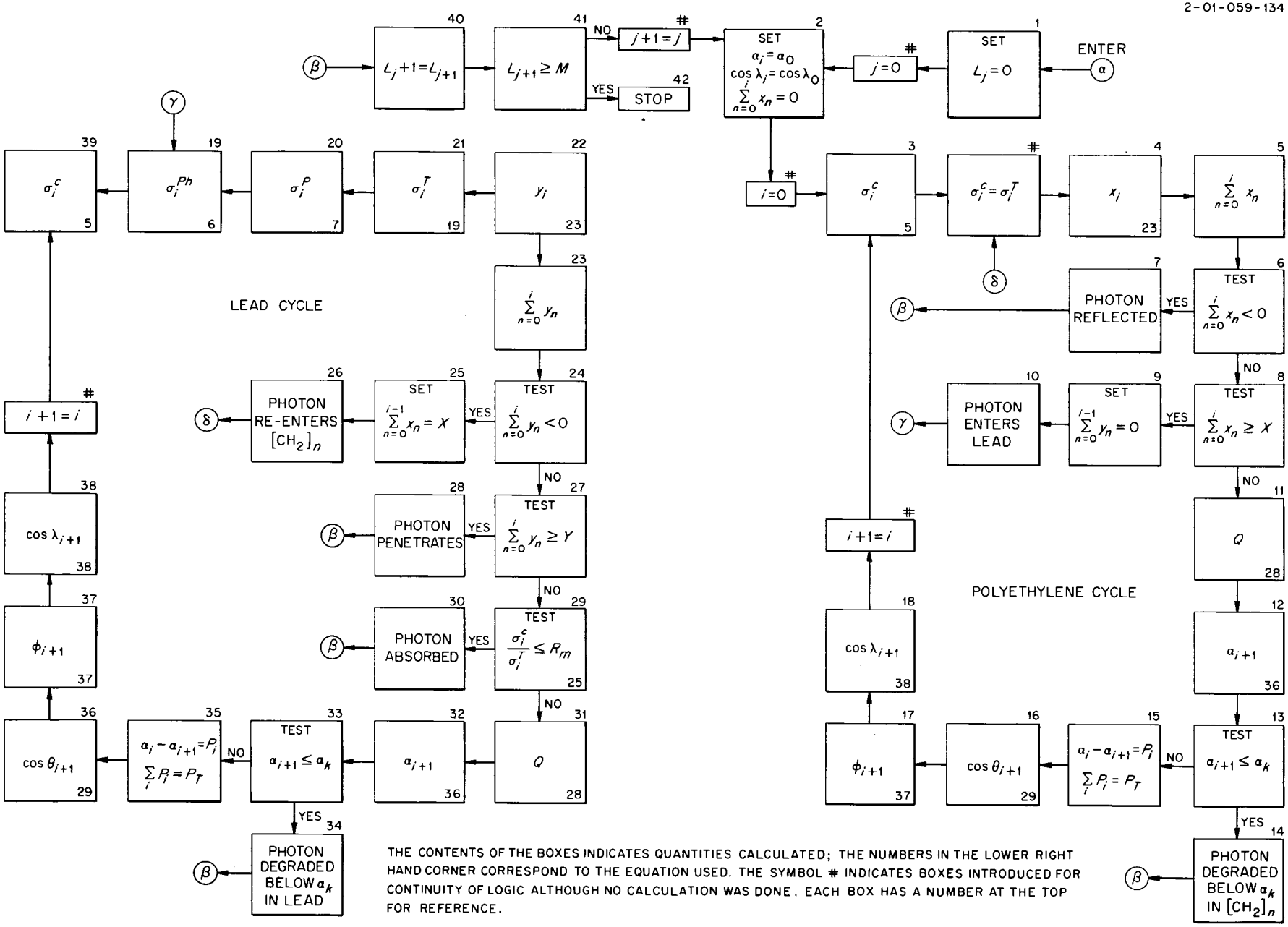


THE CONTENTS OF THE BOXES INDICATES QUANTITIES CALCULATED; THE NUMBERS IN THE LOWER RIGHT HAND CORNER CORRESPOND TO THE EQUATION USED. THE SYMBOL # INDICATES BOXES INTRODUCED FOR CONTINUITY OF LOGIC ALTHOUGH NO CALCULATION WAS DONE. EACH BOX HAS A NUMBER AT THE TOP FOR REFERENCE.

Fig. 4. Flow Diagram of Calculation for Gamma-Ray Penetration of Stratified Slab.

kept of the number of photons degraded below $\alpha_k$ in each material. A new photon history was started whenever the photon was degraded to an energy less than $\alpha_k$ or was absorbed. A new history was also started if $\sum_{n=o}^{i} x_n < 0$, which indicates the photon was reflected (block 7), or if $\sum_{n=o}^{i} y_n \geq Y$, which indicates the photon had penetrated the slab (block 28). The photon enters the lead slab when $\sum_{n=o}^{i} x_n \geq X$ (block 10), and, in this case, a transfer was made to the lead cycle and a new distance $y_i$ calculated for travel through the lead slab. The photon could again return to the polyethylene slab if $\sum_{n=o}^{i} y_i < 0$ (block 26), and similarly, a transfer was made to the polyethylene cycle and a new distance $x_i$ calculated in that material. Some typical photon histories are shown in Fig. 1.

The complete procedure corresponding to that indicated on the flow diagram was coded for calculation on the ORACLE with the additional alternatives of calculating the penetration through individual slabs of lead or polyethylene. For convenience all data was calculated as the fraction of incident photons or fraction of incident energy. The running time on the ORACLE averaged about five minutes for 1,000 sample photons.

# CHAPTER IV

## RESULTS OF CALCULATION AND DISCUSSION

### Presentation of Calculated Data

Calculations were made for a series of slabs of polyethylene, lead, and stratified slabs of a layer of polyethylene followed by a layer of lead. The transmission through the polyethylene slabs and the lead slabs was calculated primarily for comparison with other calculations and with experimental data obtained with a $Co^{60}$ source. This source emits two photons of 1.33 and 1.17 mev in equal proportions; however, in the calculation the average energy of the photons was taken which corresponds to the energy $2.45\text{-}m_oc^2$. For the stratified slabs, source energies of 2.00 and $6.00\text{-}m_oc^2$ were used. The various boundary conditions for each source energy are given in Table IV. The physical constants used for polyethylene and lead are given in Table V for purposes of comparison with other calculations or with experiment. The linear absorption cofficients given for lead in Table V were calculated using (5), (6), and (7), and those for polyethylene were calculated using (5).

The data obtained includes a detailed energy balance and photon balance. This was done to provide a check during calculation; however, since it provides a considerable amount of detail that may be of use, it is presented in Tables VI through XII. The photon distribution data was normalized to one source photon and the energy distribution was obtained as fractions of the incident energy.

TABLE IV

BOUNDARY CONDITIONS USED FOR SOLUTION OF THE PROBLEM OF TRANSMISSION OF GAMMA RADIATION THROUGH SLABS

| Photon Energy ($m_oc^2$) | Polyethylene Thickness (in.) | Lead Thickness | Angle of Incidence (deg) |
|---|---|---|---|
| 2.45 | | 0.1, 0.3, 0.5, 0.7 in. | 0, 30, 60, 75, 85 |
| | | 0.5 cm. | 75, 85 |
| | | 1.0 cm | 75, 85 |
| | | 2.5 cm | 0, 30, 60, 75, 85 |
| | | 5.0 cm | 0, 30, 60, 75 |
| | | 7.5 cm | 0, 30, 60 |
| | | 10.0 cm | 0, 30, 60 |
| 2.45 | 3 | | 0, 60 |
| | 9 | | 0, 60 |
| | 15 | | 0, 60 |
| | 30 | | 0 |
| 2, 6 | 3 | 0, 0.1, 0.3, 0.5 in. | 0, 30, 60 |
| 2, 6 | 9 | 0, 0.1, 0.3, 0.5 in. | 0. 30, 60 |
| 2, 6 | 15 | 0, 0.1, 0.3, 0.5 in. | 0, 30, 60 |

TABLE V

PHYSICAL CONSTANTS OF POLYETHYLENE AND LEAD

| Material | Composition | Density | No. of Electrons in 1 $cm^3$ | Linear Absorption Coefficient for Gamma Rays ($cm^{-1}$) | | |
|---|---|---|---|---|---|---|
| | | | | 2.00 $m_oc^2$ | 2.45 $m_oc^2$ | 6.00 $m_oc^2$ |
| Polyethylene | $(CH_2)_n$ | 1.045 | $0.3590 \times 10^{24}$ | 0.0754 | 0.0680 | 0.0406 |
| Lead | | 11.30 | $2.6936 \times 10^{24}$ | 0.7572 | 0.6527 | 0.4641 |

TABLE VI

TOTAL PHOTON AND ENERGY DISTRIBUTION OF $CO^{60}$ PHOTONS ($2.45\ m_0c^2$) SLANT INCIDENT ON A LEAD SLAB

| No. of Sample Photons | Angle of Incidence (deg) | Lead Thickness | Fraction of Incident Photons | | | | Fraction of Incident Energy | | | |
|---|---|---|---|---|---|---|---|---|---|---|
| | | | | | Penetrating Slab | | | Absorbed in Slab | | |
| | | | Reflected | Absorbed | Total | Without Degradation in Energy | Reflected | As a Result of Scattering Collisions | As a Result of Absorption Collisions | Penetrating Slab |
| 1,000 | 0 | .1 in. | 0.009 | 0.071 | 0.920 | 0.858 | 0.001993 | 0.053157 | 0.048795 | 0.896056 |
| | | .3 | 0.016 | 0.222 | 0.762 | 0.621 | 0.003438 | 0.154872 | 0.123250 | 0.718441 |
| | | .5 | 0.010 | 0.380 | 0.610 | 0.438 | 0.002008 | 0.247405 | 0.191069 | 0.559517 |
| | | .7 | 0.002 | 0.519 | 0.479 | 0.317 | 0.000435 | 0.310889 | 0.256540 | 0.432135 |
| 1,000 | 30 | .1 in. | 0.011 | 0.078 | 0.911 | 0.838 | 0.002937 | 0.054263 | 0.056569 | 0.886231 |
| | | .3 | 0.016 | 0.275 | 0.709 | 0.548 | 0.003799 | 0.188343 | 0.153409 | 0.654450 |
| | | .5 | 0.017 | 0.431 | 0.552 | 0.392 | 0.004019 | 0.274135 | 0.219054 | 0.502791 |
| | | .7 | 0.016 | 0.573 | 0.411 | 0.271 | 0.003696 | 0.325589 | 0.299971 | 0.370744 |
| 1,000 | 30 | 2.5 cm | 0.021 | 0.711 | 0.268 | 0.164 | 0.004844 | 0.410809 | 0.345523 | 0.238824 |
| | | 5.0 | 0.024 | 0.922 | 0.054 | 0.024 | 0.006530 | 0.517495 | 0.431271 | 0.044703 |
| | | 7.5 | 0.017 | 0.967 | 0.016 | 0.005 | 0.004089 | 0.520404 | 0.463070 | 0.012437 |
| | | 10.0 | 0.019 | 0.979 | 0.002 | 0.001 | 0.004641 | 0.520325 | 0.473078 | 0.001956 |
| 1,000 | 60 | .1 in. | 0.042 | 0.134 | 0.824 | 0.716 | 0.014722 | 0.112655 | 0.087007 | 0.785616 |
| | | .3 | 0.050 | 0.451 | 0.499 | 0.334 | 0.017743 | 0.291366 | 0.250429 | 0.440462 |
| | | .5 | 0.062 | 0.604 | 0.334 | 0.196 | 0.022652 | 0.366890 | 0.319935 | 0.290523 |
| | | .7 | 0.058 | 0.752 | 0.190 | 0.088 | 0.021091 | 0.435060 | 0.387352 | 0.156497 |
| 1,000 | 75 | 0.5 cm | 0.130 | 0.416 | 0.454 | 0.277 | 0.058608 | 0.310445 | 0.243643 | 0.387304 |
| | | 1.0 | 0.153 | 0.672 | 0.175 | 0.064 | 0.065042 | 0.449167 | 0.352089 | 0.133701 |
| | | 2.5 | 0.150 | 0.819 | 0.031 | 0.002 | 0.068421 | 0.499020 | 0.409334 | 0.019319 |
| | | 5.0 | 0.152 | 0.847 | 0.001 | 0.000 | 0.072172 | 0.488394 | 0.439085 | 0.000349 |
| 1,000 | 85 | .1 in. | 0.256 | 0.395 | 0.349 | 0.122 | 0.125826 | 0.364600 | 0.258041 | 0.251533 |
| | | .3 | 0.254 | 0.624 | 0.122 | 0.002 | 0.129640 | 0.448314 | 0.352594 | 0.069452 |
| | | .5 | 0.241 | 0.705 | 0.054 | 0.000 | 0.122363 | 0.449425 | 0.394584 | 0.033628 |
| | | .7 | 0.236 | 0.748 | 0.016 | 0.000 | 0.119651 | 0.463369 | 0.407919 | 0.009060 |
| 10,000 | 0 | 2.5 cm | 0.0126 | 0.6656 | 0.3218 | 0.1996 | 0.002627 | 0.374044 | 0.337036 | 0.286293 |
| | | 5.0 | 0.0127 | 0.9024 | 0.0849 | 0.0388 | 0.002680 | 0.483345 | 0.441942 | 0.072033 |
| | | 7.5 | 0.0118 | 0.9641 | 0.0241 | 0.0087 | 0.002547 | 0.508700 | 0.468634 | 0.020118 |
| | | 10.0 | 0.0135 | 0.9814 | 0.0051 | 0.0020 | 0.002866 | 0.508761 | 0.484067 | 0.004305 |
| 10,000 | 60 | 2.5 cm | 0.0567 | 0.8390 | 0.1043 | 0.0404 | 0.020552 | 0.474668 | 0.421216 | 0.083564 |
| | | 5.0 | 0.0559 | 0.9338 | 0.0103 | 0.0016 | 0.020384 | 0.507909 | 0.464208 | 0.007499 |
| | | 7.5 | 0.0567 | 0.9421 | 0.0012 | 0.0000 | 0.020781 | 0.507517 | 0.470939 | 0.000763 |
| | | 10.0 | 0.0564 | 0.9436 | 0.0000 | 0.0000 | 0.020681 | 0.508179 | 0.471140 | 0.000000 |
| 10,000 | 75 | .1 in. | 0.9870 | 0.233 | 0.6680 | 0.5089 | 0.043792 | 0.202299 | 0.147570 | 0.606340 |
| | | .3 | 0.1366 | 0.5733 | 0.2901 | 0.1347 | 0.060353 | 0.388519 | 0.320680 | 0.230448 |
| | | .5 | 0.1431 | 0.7327 | 0.1242 | 0.0341 | 0.062932 | 0.457129 | 0.390576 | 0.089362 |
| | | .7 | 0.1365 | 0.8011 | 0.0624 | 0.0076 | 0.061599 | 0.477982 | 0.418533 | 0.041886 |
| 10,000 | 85 | 0.5 cm | 0.2474 | 0.5709 | 0.1817 | 0.0245 | 0.124925 | 0.421050 | 0.399821 | 0.114204 |
| | | 1.0 | 0.2480 | 0.6775 | 0.0745 | 0.0010 | 0.125271 | 0.452618 | 0.378922 | 0.043188 |
| | | 2.5 | 0.2473 | 0.7449 | 0.0078 | 0.0000 | 0.123659 | 0.466264 | 0.405585 | 0.004492 |

TABLE VII

TOTAL PHOTON DISTRIBUTION BETWEEN 0.1727 AND 2.45 $m_oc^2$ OF $CO^{60}$ PHOTONS ($2.45\text{-}m_oc^2$) SLANT INCIDENT ON A POLYETHYLENE SLAB

| No. of Sample Photons | Angle of Incidence (deg) | Polyethylene Thickness (in.) | Fraction of Incident Photons | | | |
|---|---|---|---|---|---|---|
| | | | | | Penetrating Slab | |
| | | | Reflected | Degraded below 0.1727 $m_oc^2$ in Slab | Total | Without Degradation in Energy |
| 1000 | 0 | 3 | 0.112 | 0.019 | 0.869 | 0.602 |
| | | 9 | 0.184 | 0.256 | 0.560 | 0.227 |
| | | 15 | 0.223 | 0.488 | 0.289 | 0.072 |
| | | 30 | 0.199 | 0.765 | 0.036 | 0.003 |
| | 60 | 3 | 0.245 | 0.046 | 0.709 | 0.350 |
| | | 9 | 0.344 | 0.340 | 0.316 | 0.047 |
| | | 15 | 0.338 | 0.556 | 0.106 | 0.007 |

TABLE VIII

TOTAL ENERGY DISTRIBUTION BETWEEN 0.1727 AND 2.45 $m_oc^2$ OF $CO^{60}$ PHOTONS ($2.45 - m_oc^2$) SLANT INCIDENT ON A POLYETHYLENE SLAB

| No. of Sample Photons | Angle of Incidence (deg) | Polyethylene Thickness (in.) | Fraction of Incident Energy | | | |
|---|---|---|---|---|---|---|
| | | | Reflected | Absorbed in Slab as Result of Scattering Collisions | Degraded below 0.1727 $m_oc^2$ in Slab | Penetrating Slab |
| 1000 | 0 | 3 | 0.019698 | 0.230416 | 0.001210 | 0.748675 |
| | | 9 | 0.028961 | 0.565098 | 0.016398 | 0.389543 |
| | | 15 | 0.035432 | 0.765590 | 0.031217 | 0.167761 |
| | | 30 | 0.032452 | 0.902206 | 0.048616 | 0.016729 |
| | 60 | 3 | 0.059112 | 0.404689 | 0.002914 | 0.533285 |
| | | 9 | 0.074856 | 0.754496 | 0.021778 | 0.148870 |
| | | 15 | 0.073669 | 0.849176 | 0.035444 | 0.041712 |

TABLE IX

TOTAL PHOTON DISTRIBUTION BETWEEN 0.1727 AND 2-$m_oc^2$ OF 2-$m_oc^2$ PHOTONS SLANT INCIDENT ON A STRATIFIED SLAB OF POLYETHYLENE BACKED BY LEAD

| No. of Sample Photons | Angle of Incidence (deg) | Slab Thickness (in.) | | Fraction of Incident Photons | | | | | |
|---|---|---|---|---|---|---|---|---|---|
| | | | | | | Degraded below 0.1727 $m_oc^2$ | | Penetrating Slab | |
| | | Polyethylene | Lead | Reflected | Absorbed in Lead | In Polyethylene | In Lead | Total | Without Degradation in Energy |
| 1,000 | 0 | 3 | 0.0 | 0.124 | | 0.021 | | 0.855 | 0.569 |
| | | | 0.1 | 0.138 | 0.162 | 0.029 | 0.000 | 0.671 | 0.480 |
| | | | 0.3 | 0.135 | 0.327 | 0.039 | 0.000 | 0.499 | 0.328 |
| | | | 0.5 | 0.117 | 0.482 | 0.038 | 0.000 | 0.363 | 0.237 |
| | | 9 | 0.0 | 0.196 | | 0.302 | | 0.502 | 0.181 |
| | | | 0.1 | 0.214 | 0.189 | 0.285 | 0.001 | 0.311 | 0.159 |
| | | | 0.3 | 0.190 | 0.283 | 0.301 | 0.001 | 0.225 | 0.119 |
| | | | 0.5 | 0.205 | 0.358 | 0.302 | 0.000 | 0.135 | 0.069 |
| | | 15 | 0.0 | 0.223 | | 0.529 | | 0.248 | 0.067 |
| | | | 0.1 | 0.225 | 0.092 | 0.535 | 0.000 | 0.148 | 0.048 |
| | | | 0.3 | 0.216 | 0.155 | 0.546 | 0.000 | 0.083 | 0.027 |
| | | | 0.5 | 0.203 | 0.181 | 0.545 | 0.000 | 0.071 | 0.026 |
| | 30 | 3 | 0.0 | 0.150 | | 0.031 | | 0.819 | 0.526 |
| | | | 0.1 | 0.151 | 0.186 | 0.038 | 0.000 | 0.625 | 0.433 |
| | | | 0.3 | 0.180 | 0.357 | 0.029 | 0.000 | 0.434 | 0.299 |
| | | | 0.5 | 0.161 | 0.503 | 0.036 | 0.000 | 0.300 | 0.173 |
| | | 9 | 0.0 | 0.244 | | 0.309 | | 0.447 | 0.145 |
| | | | 0.1 | 0.232 | 0.161 | 0.323 | 0.000 | 0.284 | 0.126 |
| | | | 0.3 | 0.238 | 0.255 | 0.349 | 0.002 | 0.156 | 0.076 |
| | | | 0.5 | 0.238 | 0.323 | 0.337 | 0.001 | 0.101 | 0.045 |
| | | 15 | 0.0 | 0.273 | | 0.541 | | 0.186 | 0.030 |
| | | | 0.1 | 0.259 | 0.084 | 0.551 | 0.000 | 0.106 | 0.025 |
| | | | 0.3 | 0.256 | 0.139 | 0.544 | 0.000 | 0.061 | 0.014 |
| | | | 0.5 | 0.244 | 0.166 | 0.553 | 0.000 | 0.037 | 0.012 |
| | 60 | 3 | 0.0 | 0.259 | | 0.051 | | 0.690 | 0.315 |
| | | | 0.1 | 0.263 | 0.263 | 0.048 | 0.000 | 0.426 | 0.224 |
| | | | 0.3 | 0.289 | 0.432 | 0.046 | 0.000 | 0.233 | 0.116 |
| | | | 0.5 | 0.271 | 0.542 | 0.061 | 0.000 | 0.126 | 0.051 |
| | | 9 | 0.0 | 0.370 | | 0.356 | | 0.274 | 0.026 |
| | | | 0.1 | 0.241 | 0.157 | 0.370 | 0.002 | 0.130 | 0.026 |
| | | | 0.3 | 0.360 | 0.204 | 0.364 | 0.000 | 0.072 | 0.014 |
| | | | 0.5 | 0.362 | 0.242 | 0.361 | 0.000 | 0.035 | 0.009 |
| | | 15 | 0.0 | 0.351 | | 0.560 | | 0.089 | 0.003 |
| | | | 0.1 | 0.376 | 0.049 | 0.539 | 0.000 | 0.036 | 0.004 |
| | | | 0.3 | 0.361 | 0.074 | 0.545 | 0.000 | 0.020 | 0.003 |
| | | | 0.5 | 0.370 | 0.089 | 0.534 | 0.000 | 0.007 | 0.002 |

TABLE X

TOTAL ENERGY DISTRIBUTION BETWEEN 0.1727 AND 2-$m_oc^2$ OF 2-$m_oc^2$ PHOTONS SLANT INCIDENT ON A STRATIFIED SLAB OF POLYETHYLENE BACKED BY LEAD

| No. of Sample Photons | Angle of Incidence (deg) | Slab Thickness (in.) | | Fraction of Incident Energy | | | | | | |
|---|---|---|---|---|---|---|---|---|---|---|
| | | | | | Absorbed as Result of Scattering Collisions | | Absorbed in Lead as Result of Absorption Collisions | Degraded below 0.1727 $m_oc^2$ | | |
| | | Polyethylene | Lead | Reflected | In Polyethrylene | In Lead | | In Polyethylene | In Lead | Penetrating Slab |
| 1000 | 0 | 3 | 0.0 | 0.024715 | 0.239791 | | | 0.001639 | | 0.733855 |
| | | | 0.1 | 0.029116 | 0.242090 | 0.047604 | 0.064712 | 0.002321 | 0.000000 | 0.614158 |
| | | | 0.3 | 0.027565 | 0.249937 | 0.115757 | 0.155091 | 0.003143 | 0.000000 | 0.448506 |
| | | | 0.5 | 0.024853 | 0.239460 | 0.173041 | 0.232553 | 0.003031 | 0.000000 | 0.327062 |
| | | 9 | 0.0 | 0.037845 | 0.591109 | | | 0.023355 | | 0.347692 |
| | | | 0.1 | 0.041217 | 0.589380 | 0.026970 | 0.056317 | 0.022283 | 0.000076 | 0.263757 |
| | | | 0.3 | 0.036195 | 0.585592 | 0.062297 | 0.097851 | 0.023442 | 0.000076 | 0.194547 |
| | | | 0.5 | 0.039278 | 0.599699 | 0.088169 | 0.131643 | 0.023501 | 0.000000 | 0.117709 |
| | | 15 | 0.0 | 0.042681 | 0.766765 | | | 0.041263 | | 0.149280 |
| | | | 0.1 | 0.041918 | 0.768146 | 0.006480 | 0.024711 | 0.041828 | 0.000000 | 0.116916 |
| | | | 0.3 | 0.040609 | 0.774999 | 0.021743 | 0.052655 | 0.042643 | 0.000000 | 0.067351 |
| | | | 0.5 | 0.037688 | 0.764803 | 0.030084 | 0.065639 | 0.042540 | 0.000000 | 0.059247 |
| | 30 | 3 | 0.0 | 0.032782 | 0.272493 | | | 0.002440 | | 0.692285 |
| | | | 0.1 | 0.034267 | 0.284645 | 0.044554 | 0.067588 | 0.002992 | 0.000000 | 0.565954 |
| | | | 0.3 | 0.040221 | 0.281790 | 0.113269 | 0.166510 | 0.002282 | 0.000000 | 0.395927 |
| | | | 0.5 | 0.035328 | 0.285609 | 0.169844 | 0.240003 | 0.002864 | 0.000000 | 0.266352 |
| | | 9 | 0.0 | 0.049868 | 0.637456 | | | 0.024114 | | 0.288561 |
| | | | 0.1 | 0.048014 | 0.626108 | 0.020692 | 0.048982 | 0.025358 | 0.000000 | 0.230846 |
| | | | 0.3 | 0.045817 | 0.658672 | 0.045178 | 0.090106 | 0.027345 | 0.000169 | 0.132714 |
| | | | 0.5 | 0.045794 | 0.658724 | 0.066276 | 0.118202 | 0.026189 | 0.000084 | 0.084731 |
| | | 15 | 0.0 | 0.056388 | 0.803700 | | | 0.042009 | | 0.097903 |
| | | | 0.1 | 0.051850 | 0.796393 | 0.004086 | 0.024566 | 0.043045 | 0.000000 | 0.080061 |
| | | | 0.3 | 0.052141 | 0.789485 | 0.015233 | 0.051105 | 0.042519 | 0.000000 | 0.049517 |
| | | | 0.5 | 0.047990 | 0.792782 | 0.021988 | 0.062974 | 0.043096 | 0.000000 | 0.031170 |
| | 60 | 3 | 0.0 | 0.073676 | 0.413683 | | | 0.003938 | | 0.508703 |
| | | | 0.1 | 0.073205 | 0.408444 | 0.057714 | 0.103061 | 0.003768 | 0.000000 | 0.353808 |
| | | | 0.3 | 0.083293 | 0.418549 | 0.123567 | 0.175824 | 0.003638 | 0.000000 | 0.195129 |
| | | | 0.5 | 0.078946 | 0.414278 | 0.166778 | 0.233599 | 0.004745 | 0.000000 | 0.101654 |
| | | 9 | 0.0 | 0.092467 | 0.757028 | | | 0.027875 | | 0.122630 |
| | | | 0.1 | 0.085171 | 0.744772 | 0.012269 | 0.037249 | 0.028845 | 0.000166 | 0.091528 |
| | | | 0.3 | 0.089741 | 0.748754 | 0.024082 | 0.058722 | 0.028417 | 0.000000 | 0.050284 |
| | | | 0.5 | 0.090885 | 0.747751 | 0.031359 | 0.076503 | 0.028167 | 0.000000 | 0.025336 |
| | | 15 | 0.0 | 0.088710 | 0.835702 | | | 0.043596 | | 0.031991 |
| | | | 0.1 | 0.097495 | 0.822561 | 0.002516 | 0.011963 | 0.042032 | 0.000000 | 0.023483 |
| | | | 0.3 | 0.089779 | 0.830431 | 0.005470 | 0.019128 | 0.042546 | 0.000000 | 0.012645 |
| | | | 0.5 | 0.090956 | 0.829881 | 0.005430 | 0.026302 | 0.0415901 | 0.000000 | 0.005840 |

TABLE XI

TOTAL PHOTON DISTRIBUTION BETWEEN ENERGY 0.1727 AND 6-$m_oc^2$ OF 6-$m_oc^2$ PHOTONS SLANT INCIDENT ON A STRATIFIED SLAB OF POLYETHYLENE BACKED BY LEAD

| No. of Sample Photons | Angle of Incidence (deg) | Slab Thickness (in.) | | Fraction of Incident Photons | | | | | |
|---|---|---|---|---|---|---|---|---|---|
| | | | | | | Degraded below 0.1727 $m_oc^2$ | | Penetrating Slab | |
| | | Polyethylene | Lead | Reflected | Absorbed in Lead | Polyethylene | Lead | Total | Without Degradation in Energy |
| 1000 | 0 | 3 | 0.0 | 0.071 | | 0.011 | | 0.918 | 0.727 |
| | | | 0.1 | 0.070 | 0.091 | 0.008 | 0.000 | 0.831 | 0.650 |
| | | | 0.3 | 0.068 | 0.202 | 0.014 | 0.000 | 0.716 | 0.525 |
| | | | 0.5 | 0.073 | 0.306 | 0.009 | 0.000 | 0.612 | 0.426 |
| | | 9 | 0.0 | 0.126 | | 0.152 | | 0.722 | 0.397 |
| | | | 0.1 | 0.123 | 0.110 | 0.178 | 0.000 | 0.589 | 0.361 |
| | | | 0.3 | 0.126 | 0.213 | 0.157 | 0.000 | 0.504 | 0.287 |
| | | | 0.5 | 0.113 | 0.283 | 0.178 | 0.000 | 0.426 | 0.229 |
| | | 15 | 0.0 | 0.119 | | 0.338 | | 0.543 | 0.227 |
| | | | 0.1 | 0.113 | 0.106 | 0.366 | 0.000 | 0.415 | 0.203 |
| | | | 0.3 | 0.115 | 0.181 | 0.349 | 0.001 | 0.354 | 0.170 |
| | | | 0.5 | 0.127 | 0.231 | 0.367 | 0.000 | 0.275 | 0.130 |
| | 30 | 3 | 0.0 | 0.081 | | 0.010 | | 0.909 | 0.701 |
| | | | 0.1 | 0.098 | 0.102 | 0.021 | 0.000 | 0.779 | 0.594 |
| | | | 0.3 | 0.082 | 0.239 | 0.009 | 0.000 | 0.670 | 0.489 |
| | | | 0.5 | 0.080 | 0.344 | 0.016 | 0.000 | 0.560 | 0.368 |
| | | 9 | 0.0 | 0.153 | | 0.164 | | 0.683 | 0.349 |
| | | | 0.1 | 0.149 | 0.120 | 0.182 | 0.000 | 0.549 | 0.300 |
| | | | 0.3 | 0.158 | 0.212 | 0.191 | 0.001 | 0.438 | 0.241 |
| | | | 0.5 | 0.144 | 0.332 | 0.184 | 0.001 | 0.339 | 0.186 |
| | | 15 | 0.0 | 0.147 | | 0.397 | | 0.456 | 0.164 |
| | | | 0.1 | 0.162 | 0.093 | 0.399 | 0.001 | 0.345 | 0.146 |
| | | | 0.3 | 0.162 | 0.159 | 0.404 | 0.000 | 0.275 | 0.121 |
| | | | 0.5 | 0.159 | 0.229 | 0.388 | 0.000 | 0.224 | 0.085 |
| | 60 | 3 | 0.0 | 0.149 | | 0.015 | | 0.836 | 0.546 |
| | | | 0.1 | 0.172 | 0.148 | 0.016 | 0.000 | 0.664 | 0.435 |
| | | | 0.3 | 0.167 | 0.323 | 0.024 | 0.000 | 0.486 | 0.295 |
| | | | 0.5 | 0.186 | 0.475 | 0.022 | 0.000 | 0.317 | 0.168 |
| | | 9 | 0.0 | 0.257 | | 0.258 | | 0.485 | 0.144 |
| | | | 0.1 | 0.255 | 0.137 | 0.257 | 0.000 | 0.351 | 0.130 |
| | | | 0.3 | 0.237 | 0.281 | 0.262 | 0.000 | 0.220 | 0.081 |
| | | | 0.5 | 0.263 | 0.322 | 0.247 | 0.000 | 0.168 | 0.055 |
| | | 15 | 0.0 | 0.271 | | 0.472 | | 0.257 | 0.050 |
| | | | 0.1 | 0.291 | 0.089 | 0.454 | 0.001 | 0.165 | 0.032 |
| | | | 0.3 | 0.267 | 0.163 | 0.468 | 0.000 | 0.102 | 0.021 |
| | | | 0.5 | 0.253 | 0.190 | 0.484 | 0.000 | 0.073 | 0.015 |

TABLE XII

TOTAL ENERGY DISTRIBUTION BETWEEN 0.1727 AND 6-$m_oc^2$ OF 6-$m_oc^2$ PHOTONS SLANT INCIDENT ON A STRATIFIED SLAB OF POLYETHYLENE BACKED BY LEAD

| No. of Sample Photons | Angle of Incidence (deg) | Slab Thickness (in.) | | Fraction of Incident Energy | | | | | | |
|---|---|---|---|---|---|---|---|---|---|---|
| | | | | | Absorbed as Result of Scattering Collisions | | Absorbed in Lead as Result of Absorption Collisions | Degraded below 0.1727 $m_oc^2$ | | |
| | | Polyethylene | Lead | Reflected | In Polyethylene | In Lead | | In Polyethylene | In Lead | Penetrating Slab |
| 1000 | 0 | 3 | 0.0 | 0.006134 | 0.178874 | | | 0.000288 | | 0.814703 |
| | | | 0.1 | 0.005644 | 0.176245 | 0.038820 | 0.031180 | 0.000212 | 0.000000 | 0.747898 |
| | | | 0.3 | 0.005684 | 0.168406 | 0.102296 | 0.096321 | 0.000375 | 0.000000 | 0.626918 |
| | | | 0.5 | 0.006244 | 0.175673 | 0.156327 | 0.135921 | 0.000233 | 0.000000 | 0.525601 |
| | | 9 | 0.0 | 0.009199 | 0.446106 | | | 0.003934 | | 0.540761 |
| | | | 0.1 | 0.009304 | 0.448568 | 0.022925 | 0.031416 | 0.004643 | 0.000000 | 0.483144 |
| | | | 0.3 | 0.009667 | 0.451032 | 0.071090 | 0.061331 | 0.004097 | 0.000000 | 0.402783 |
| | | | 0.5 | 0.008470 | 0.452938 | 0.100517 | 0.096212 | 0.004641 | 0.000000 | 0.337222 |
| | | 15 | 0.0 | 0.008306 | 0.631807 | | | 0.008786 | | 0.351100 |
| | | | 0.1 | 0.008244 | 0.633816 | 0.015169 | 0.018691 | 0.009568 | 0.000000 | 0.314511 |
| | | | 0.3 | 0.008323 | 0.617308 | 0.044238 | 0.046138 | 0.009082 | 0.000027 | 0.274884 |
| | | | 0.5 | 0.009090 | 0.625673 | 0.078003 | 0.067594 | 0.009524 | 0.000000 | 0.210116 |
| | 30 | 3 | 0.0 | 0.007262 | 0.198385 | | | 0.000267 | | 0.794087 |
| | | | 0.1 | 0.009331 | 0.214009 | 0.042804 | 0.039768 | 0.000561 | 0.000000 | 0.693527 |
| | | | 0.3 | 0.007262 | 0.185937 | 0.11457 | 0.103330 | 0.000240 | 0.000000 | 0.591774 |
| | | | 0.5 | 0.007220 | 0.196112 | 0.166901 | 0.155299 | 0.000422 | 0.000000 | 0.474045 |
| | | 9 | 0.0 | 0.012143 | 0.491480 | | | 0.004263 | | 0.492114 |
| | | | 0.1 | 0.011481 | 0.501139 | 0.032962 | 0.021187 | 0.004765 | 0.000000 | 0.428465 |
| | | | 0.3 | 0.012546 | 0.506400 | 0.068854 | 0.062608 | 0.005032 | 0.000025 | 0.344535 |
| | | | 0.5 | 0.011611 | 0.503180 | 0.119450 | 0.093504 | 0.004822 | 0.000025 | 0.267408 |
| | | 15 | 0.0 | 0.011195 | 0.696598 | | | 0.010240 | | 0.281967 |
| | | | 0.1 | 0.012492 | 0.691657 | 0.013321 | 0.018688 | 0.010422 | 0.000028 | 0.253391 |
| | | | 0.3 | 0.012657 | 0.691764 | 0.038698 | 0.040230 | 0.010497 | 0.000000 | 0.206155 |
| | | | 0.5 | 0.012518 | 0.685720 | 0.072430 | 0.057339 | 0.010075 | 0.000000 | 0.161917 |
| | 60 | 3 | 0.0 | 0.018229 | 0.313678 | | | 0.000393 | | 0.667700 |
| | | | 0.1 | 0.023441 | 0.317884 | 0.056831 | 0.051074 | 0.000430 | 0.000000 | 0.550341 |
| | | | 0.3 | 0.022127 | 0.314638 | 0.141965 | 0.130780 | 0.000624 | 0.000000 | 0.389866 |
| | | | 0.5 | 0.025081 | 0.326403 | 0.208691 | 0.193173 | 0.000572 | 0.000000 | 0.246081 |
| | | 9 | 0.0 | 0.028432 | 0.701639 | | | 0.006723 | | 0.263206 |
| | | | 0.1 | 0.025431 | 0.691915 | 0.021256 | 0.024806 | 0.006691 | 0.000000 | 0.229900 |
| | | | 0.3 | 0.024644 | 0.685401 | 0.067004 | 0.067548 | 0.006858 | 0.000000 | 0.148545 |
| | | | 0.5 | 0.028224 | 0.688364 | 0.088128 | 0.083381 | 0.006469 | 0.000000 | 0.105434 |
| | | 15 | 0.0 | 0.029151 | 0.848308 | | | 0.012272 | | 0.110269 |
| | | | 0.1 | 0.031274 | 0.846104 | 0.011982 | 0.011576 | 0.011738 | 0.000029 | 0.087296 |
| | | | 0.3 | 0.027742 | 0.851698 | 0.024762 | 0.026282 | 0.012158 | 0.000000 | 0.057359 |
| | | | 0.5 | 0.026722 | 0.848279 | 0.036337 | 0.032459 | 0.012544 | 0.000000 | 0.043658 |

For any problem the sum of the fractional distribution of photons or energy will add to one with errors due to round off the numbers only. The photon balance includes the fraction reflected, degraded below the energy corresponding to the K-edge of lead ($0.1727\text{-}m_oc^2$), penetrating the slab, and penetrating the slab without degradation (uncollided). The energy balance includes the fraction reflected, absorbed as a result of scattering collisions, absorbed as a result of absorption collisions (photoelectric and pair-production interactions), degraded below the K-edge of lead, and penetrating the slab.

It should be pointed out that the cut off energy of $0.1727\text{-}m_oc^2$ does have an influence on the interpretation of the photon and energy distribution in many cases since the photons were considered absorbed below that energy. For the polyethylene slabs, the fraction of the energy penetrating and reflected as well as the fraction of the photons penetrating and reflected could be changed by a large factor if the low energy photons were not neglected. In those cases involving lead slabs, the fractions degraded below the K-edge of lead was zero in every case and, therefore, was not included in Table VI. This means the photon and energy distributions for the lead slabs was not influenced by the cut off energy and represents estimates for the complete energy range. For the stratified slabs, the photon and energy fractions reflected could be altered by a large factor if the lower energy photons had been allowed to contribute; however, the penetration data will not be changed because of the insignificant probability that a low energy photon would penetrate the lead.

The energy spectrum of degraded photons transmitted through the stratified slabs is given in Tables XIII through XVIII.

## Accuracy of the Calculation

The accuracy of the calculation can be separated into three parts: first, the accuracy of the physical data, second, the numerical accuracy, and third, the statistical accuracy. The first has been described in Chap. II. Once the values of the physical quantities were given, the numerical error was maintained less than $10^{-6}$ in the process of all machine computation. Actually, the energy balance was maintained with error less than $10^{-12}$. The number of significant figures indicated in Tables VI through XVIII reflect the numerical accuracy only. The statistical accuracy of the estimates needs to be discussed at more length.

Each calculation was statistically independent in the sense that an independent set of photon histories was generated for each set of boundary conditions. The photons for a given set of boundary conditions form a multinomial distribution where the fraction of photons falling in each class of the distribution has an estimated variance, $\sigma^2$, given by[40]

$$\sigma^2 = \frac{F(1 - F)}{N - 1} \tag{39}$$

where

F = the estimated fraction of the photons entering the class,

---

[40] A. M. Mood, Introduction to the Theory of Statistics, (McGraw-Hill Publishing Company, Inc., New York, 1950), p. 156.

TABLE XIII

DEGRADED ENERGY SPECTRUM OF TRANSMITTED PHOTONS AS FRACTION OF 2-$m_oc^2$ PHOTONS INCIDENT AT 0 DEG ON STRATIFIED SLABS (EACH CASE HAD 1000 SAMPLE PHOTONS)

| Energy Interval $m_oc^2$ | 3 in. Polyethylene | | | | 9 in. Polyethylene | | | | 15 in. Polyethylene | | | |
|---|---|---|---|---|---|---|---|---|---|---|---|---|
| | Lead Thickness (in.) | | | | Lead Thickness (in.) | | | | Lead Thickness (in.) | | | |
| | 0 | 0.1 | 0.3 | 0.5 | 0 | 0.1 | 0.3 | 0.5 | 0 | 0.1 | 0.3 | 0.5 |
| .1727-0.2 | 0.005 | 0 | 0 | 0 | 0.012 | 0 | 0 | 0 | 0.014 | 0 | 0 | 0 |
| 0.2-0.3 | 0.027 | 0 | 0 | 0 | 0.032 | 0 | 0 | 0 | 0.027 | 0 | 0 | 0 |
| 0.3-0.4 | 0.011 | 0.001 | 0 | 0 | 0.025 | 0 | 0 | 0 | 0.012 | 0 | 0 | 0 |
| 0.4-0.5 | 0.010 | 0.002 | 0 | 0 | 0.017 | 0.003 | 0 | 0.001 | 0.005 | 0 | 0 | 0 |
| 0.5-0.6 | 0.009 | 0.006 | 0.002 | 0.002 | 0.010 | 0.002 | 0.001 | 0.002 | 0.008 | 0.002 | 0 | 0 |
| 0.6-0.7 | 0.007 | 0.004 | 0.002 | 0.005 | 0.008 | 0.001 | 0.001 | 0 | 0.009 | 0.006 | 0 | 0.001 |
| 0.7-0.8 | 0.005 | 0.002 | 0.005 | 0.002 | 0.012 | 0.005 | 0.002 | 0.001 | 0.009 | 0.004 | 0 | 0 |
| 0.8-0.9 | 0.019 | 0.008 | 0.003 | 0.003 | 0.017 | 0.006 | 0.006 | 0.003 | 0.007 | 0.002 | 0.001 | 0.002 |
| 0.9-1.0 | 0.016 | 0.010 | 0.016 | 0.006 | 0.015 | 0.008 | 0.005 | 0 | 0.008 | 0.006 | 0.001 | 0.002 |
| 1.0-1.1 | 0.015 | 0.009 | 0.011 | 0.006 | 0.018 | 0.009 | 0.011 | 0.007 | 0.013 | 0.007 | 0.003 | 0.002 |
| 1.1-1.2 | 0.016 | 0.009 | 0.007 | 0.005 | 0.021 | 0.009 | 0.006 | 0.003 | 0.008 | 0.005 | 0.001 | 0.003 |
| 1.2-1.3 | 0.017 | 0.018 | 0.017 | 0.015 | 0.010 | 0.021 | 0.008 | 0.007 | 0.009 | 0.008 | 0.005 | 0.003 |
| 1.3-1.4 | 0.013 | 0.016 | 0.016 | 0.013 | 0.024 | 0.015 | 0.008 | 0.001 | 0.011 | 0.013 | 0.002 | 0.004 |
| 1.4-1.5 | 0.021 | 0.022 | 0.013 | 0.011 | 0.019 | 0.014 | 0.008 | 0.004 | 0.004 | 0.005 | 0.004 | 0.006 |
| 1.5-1.6 | 0.015 | 0.013 | 0.024 | 0.010 | 0.018 | 0.014 | 0.009 | 0.006 | 0.013 | 0.010 | 0.005 | 0.005 |
| 1.6-1.7 | 0.023 | 0.014 | 0.016 | 0.014 | 0.017 | 0.012 | 0.013 | 0.005 | 0.006 | 0.005 | 0.004 | 0.004 |
| 1.7-1.8 | 0.021 | 0.023 | 0.012 | 0.008 | 0.016 | 0.009 | 0.009 | 0.008 | 0.004 | 0.006 | 0.004 | 0.003 |
| 1.8-1.9 | 0.020 | 0.020 | 0.013 | 0.017 | 0.010 | 0.010 | 0.007 | 0.010 | 0.002 | 0.010 | 0.005 | 0.005 |
| 1.9-2.0 | 0.016 | 0.014 | 0.014 | 0.009 | 0.020 | 0.014 | 0.012 | 0.008 | 0.002 | 0.011 | 0.006 | 0.005 |

TABLE XIV

DEGRADED ENERGY SPECTRUM OF TRANSMITTED PHOTONS AS FRACTION OF 2-$m_oc^2$ PHOTONS INCIDENT AT 30 DEG ON STRATIFIED SLABS (EACH CASE HAD 1000 SAMPLE PHOTONS)

| Energy Interval $m_oc^2$ | 3 in. Polyethylene | | | | 9 in. Polyethylene | | | | 15 in. Polyethylene | | | |
|---|---|---|---|---|---|---|---|---|---|---|---|---|
| | Lead Thickness (in.) | | | | Lead Thickness (in.) | | | | Lead Thickness (in.) | | | |
| | 0 | 0.1 | 0.3 | 0.5 | 0 | 0.1 | 0.3 | 0.5 | 0 | 0.1 | 0.3 | 0.5 |
| .1727-0.2 | 0.002 | 0 | 0 | 0 | 0.012 | 0 | 0 | 0 | 0.014 | 0 | 0 | 0 |
| 0.2-0.3 | 0.025 | 0 | 0 | 0 | 0.043 | 0 | 0 | 0 | 0.025 | 0 | 0 | 0 |
| 0.3-0.4 | 0.015 | 0.002 | 0 | 0 | 0.027 | 0 | 0 | 0 | 0.012 | 0 | 0 | 0 |
| 0.4-0.5 | 0.010 | 0.004 | 0 | 0 | 0.020 | 0.004 | 0 | 0 | 0.006 | 0.003 | 0 | 0 |
| 0.5-0.6 | 0.008 | 0.003 | 0.001 | 0 | 0.012 | 0.003 | 0.001 | 0 | 0.008 | 0.001 | 0 | 0 |
| 0.6-0.7 | 0.018 | 0.001 | 0.002 | 0.004 | 0.013 | 0.002 | 0.001 | 0.002 | 0.006 | 0.003 | 0 | 0 |
| 0.7-0.8 | 0.006 | 0.005 | 0.003 | 0.002 | 0.010 | 0.005 | 0 | 0.002 | 0.008 | 0.001 | 0 | 0 |
| 0.8-0.9 | 0.016 | 0.009 | 0.002 | 0.006 | 0.017 | 0.014 | 0.003 | 0.003 | 0.008 | 0.004 | 0.001 | 0 |
| 0.9-1.0 | 0.018 | 0.009 | 0.007 | 0.004 | 0.012 | 0.007 | 0.004 | 0.004 | 0.006 | 0.004 | 0.002 | 0.002 |
| 1.0-1.1 | 0.018 | 0.015 | 0.013 | 0.008 | 0.011 | 0.018 | 0.009 | 0.004 | 0.008 | 0.006 | 0.002 | 0.002 |
| 1.1-1.2 | 0.013 | 0.015 | 0.008 | 0.005 | 0.014 | 0.007 | 0.006 | 0.002 | 0.005 | 0.006 | 0.005 | 0 |
| 1.2-1.3 | 0.019 | 0.014 | 0.010 | 0.009 | 0.011 | 0.011 | 0.005 | 0.002 | 0.007 | 0.005 | 0.004 | 0.002 |
| 1.3-1.4 | 0.014 | 0.011 | 0.011 | 0.010 | 0.016 | 0.011 | 0.006 | 0.004 | 0.004 | 0.007 | 0.004 | 0.004 |
| 1.4-1.5 | 0.020 | 0.019 | 0.008 | 0.006 | 0.014 | 0.015 | 0.009 | 0.004 | 0.007 | 0.010 | 0.002 | 0 |
| 1.5-1.6 | 0.016 | 0.019 | 0.018 | 0.019 | 0.010 | 0.019 | 0.008 | 0.007 | 0.008 | 0.007 | 0.006 | 0.004 |
| 1.6-1.7 | 0.017 | 0.016 | 0.020 | 0.016 | 0.015 | 0.009 | 0.009 | 0.007 | 0.008 | 0.003 | 0.005 | 0.001 |
| 1.7-1.8 | 0.022 | 0.014 | 0.011 | 0.012 | 0.013 | 0.013 | 0.009 | 0.005 | 0.005 | 0.005 | 0.004 | 0.003 |
| 1.8-1.9 | 0.023 | 0.022 | 0.014 | 0.014 | 0.014 | 0.009 | 0.007 | 0.005 | 0.003 | 0.007 | 0.005 | 0 |
| 1.9-2.0 | 0.013 | 0.014 | 0.007 | 0.012 | 0.018 | 0.011 | 0.003 | 0.005 | 0.008 | 0.009 | 0.007 | 0.007 |

TABLE XV

DEGRADED ENERGY SPECTRUM OF TRANSMITTED PHOTONS AS FRACTION OF 2-$m_oc^2$
PHOTONS INCIDENT AT 60 DEG ON STRATIFIED SLABS
(EACH CASE HAD 1000 SAMPLE PHOTONS

| Energy Interval $m_oc^2$ | 3 in. Polyethylene | | | | 9 in. Polyethylene | | | | 15 in. Polyethylene | | | |
|---|---|---|---|---|---|---|---|---|---|---|---|---|
| | Lead Thickness (in.) | | | | Lead Thickness (in.) | | | | Lead Thickness (in.) | | | |
| | 0 | 0.1 | 0.3 | 0.5 | 0 | 0.1 | 0.3 | 0.5 | 0 | 0.1 | 0.3 | 0.5 |
| .1727-0.2 | 0.009 | 0 | 0 | 0 | 0.011 | 0 | 0 | 0 | 0.009 | 0 | 0 | 0 |
| 0.2-0.3 | 0.028 | 0 | 0 | 0 | 0.037 | 0 | 0 | 0 | 0.018 | 0 | 0 | 0 |
| 0.3-0.4 | 0.023 | 0.001 | 0 | 0 | 0.026 | 0 | 0 | 0 | 0.011 | 0.001 | 0 | 0 |
| 0.4-0.5 | 0.018 | 0.002 | 0 | 0.002 | 0.021 | 0.002 | 0 | 0.0010 | 0.006 | 0 | 0 | 0 |
| 0.5-0.6 | 0.024 | 0.010 | 0.002 | 0.002 | 0.014 | 0.003 | 0.001 | 0 | 0.005 | 0 | 0 | 0 |
| 0.6-0.7 | 0.023 | 0.009 | 0.003 | 0.001 | 0.019 | 0.005 | 0.004 | 0.0010 | 0.005 | 0.001 | 0.001 | 0 |
| 0.7-0.8 | 0.020 | 0.012 | 0.007 | 0.005 | 0.013 | 0.005 | 0.003 | 0.0010 | 0.002 | 0.004 | 0.004 | 0 |
| 0.8-0.9 | 0.016 | 0.014 | 0.007 | 0.003 | 0.017 | 0.007 | 0.003 | 0.0020 | 0.005 | 0.003 | 0 | 0 |
| 0.9-1.0 | 0.027 | 0.010 | 0.004 | 0.002 | 0.010 | 0.006 | 0.005 | 0.0010 | 0.002 | 0.003 | 0.001 | 0 |
| 1.0-1.1 | 0.015 | 0.014 | 0.006 | 0.005 | 0.019 | 0.009 | 0.006 | 0.0010 | 0.006 | 0 | 0.003 | 0 |
| 1.1-1.2 | 0.021 | 0.011 | 0.011 | 0.006 | 0.008 | 0.010 | 0.004 | 0.0010 | 0.004 | 0.004 | 0.002 | 0.001 |
| 1.2-1.3 | 0.021 | 0.017 | 0.011 | 0.006 | 0.008 | 0.005 | 0.005 | 0.0020 | 0.001 | 0.002 | 0.002 | 0.001 |
| 1.3-1.4 | 0.021 | 0.012 | 0.013 | 0.006 | 0.006 | 0.006 | 0.003 | 0.0030 | 0.003 | 0.004 | 0.001 | 0 |
| 1.4-1.5 | 0.019 | 0.013 | 0.009 | 0.005 | 0.010 | 0.015 | 0.012 | 0.0100 | 0.001 | 0.003 | 0.001 | 0.001 |
| 1.5-1.6 | 0.019 | 0.016 | 0.008 | 0.008 | 0.012 | 0.011 | 0.004 | 0.0020 | 0 | 0.001 | 0 | 0 |
| 1.6-1.7 | 0.013 | 0.018 | 0.008 | 0.004 | 0.005 | 0.005 | 0 | 0 | 0.002 | 0.001 | 0 | 0 |
| 1.7-1.8 | 0.020 | 0.018 | 0.010 | 0.004 | 0.003 | 0.004 | 0.002 | 0 | 0.001 | 0.002 | 0 | 0 |
| 1.8-1.9 | 0.019 | 0.014 | 0.011 | 0.012 | 0.003 | 0.006 | 0.003 | 0.0010 | 0.002 | 0.001 | 0 | 0.001 |
| 1.9-2.0 | 0.019 | 0.011 | 0.007 | 0.004 | 0.006 | 0.005 | 0.003 | 0 | 0.003 | 0.002 | 0.002 | 0.001 |

TABLE XVI

DEGRADED ENERGY SPECTRUM OF TRANSMITTED PHOTONS AS FRACTION OF 6-$m_oc^2$ PHOTONS INCIDENT AT 0 DEG ON STRATIFIED SLABS
(EACH CASE HAD 1000 SAMPLE PHOTONS)

| Energy Interval $m_oc^2$ | 3 in. Polyethylene | | | | 9 in. Polyethylene | | | | 15 in. Polyethylene | | | |
|---|---|---|---|---|---|---|---|---|---|---|---|---|
| | Lead Thickness (in.) | | | | Lead Thickness (in.) | | | | Lead Thickness (in.) | | | |
| | 0 | 0.1 | 0.3 | 0.5 | 0 | 0.1 | 0.3 | 0.5 | 0 | 0.1 | 0.3 | 0.5 |
| .1727-0.2 | 0 | 0 | 0 | 0 | 0.004 | 0 | 0 | 0 | 0.006 | 0 | 0 | 0 |
| 0.2-0.4 | 0.015 | 0 | 0 | 0 | 0.030 | 0 | 0 | 0 | 0.040 | 0 | 0 | 0 |
| 0.4-0.6 | 0.014 | 0.001 | 0.002 | 0.001 | 0.020 | 0 | 0.001 | 0 | 0.028 | 0.003 | 0.001 | 0 |
| 0.6-0.8 | 0.005 | 0.001 | 0.002 | 0.001 | 0.014 | 0.013 | 0.003 | 0.001 | 0.008 | 0.004 | 0.005 | 0.001 |
| 0.8-1.0 | 0.006 | 0.002 | 0.004 | 0.005 | 0.008 | 0.005 | 0.004 | 0.002 | 0.015 | 0.010 | 0.002 | 0.002 |
| 1.0-1.2 | 0.006 | 0.008 | 0.004 | 0.002 | 0.012 | 0.006 | 0.009 | 0.007 | 0.012 | 0.008 | 0.004 | 0.002 |
| 1.2-1.4 | 0.010 | 0.009 | 0.005 | 0.004 | 0.011 | 0.005 | 0.010 | 0.006 | 0.014 | 0.008 | 0.009 | 0.006 |
| 1.4-1.6 | 0.005 | 0.009 | 0.011 | 0.007 | 0.012 | 0.016 | 0.010 | 0.007 | 0.010 | 0.007 | 0.005 | 0.008 |
| 1.6-1.8 | 0.006 | 0.008 | 0.007 | 0.009 | 0.011 | 0.010 | 0.006 | 0.009 | 0.013 | 0.009 | 0.006 | 0.007 |
| 1.8-2.0 | 0.006 | 0.011 | 0.012 | 0.014 | 0.014 | 0.008 | 0.017 | 0.008 | 0.011 | 0.008 | 0.008 | 0.003 |
| 2.0-2.2 | 0.009 | 0.006 | 0.011 | 0.012 | 0.012 | 0.010 | 0.012 | 0.014 | 0.013 | 0.018 | 0.008 | 0.009 |
| 2.2-2.4 | 0.010 | 0.009 | 0.010 | 0.010 | 0.010 | 0.006 | 0.007 | 0.011 | 0.011 | 0.006 | 0.006 | 0.011 |
| 2.4-2.6 | 0.007 | 0.005 | 0.012 | 0.008 | 0.010 | 0.009 | 0.008 | 0.017 | 0.008 | 0.008 | 0.006 | 0.008 |
| 2.6-2.8 | 0.004 | 0.008 | 0.006 | 0.014 | 0.010 | 0.008 | 0.008 | 0.007 | 0.006 | 0.009 | 0.007 | 0.006 |
| 2.8-3.0 | 0.006 | 0.006 | 0.004 | 0.006 | 0.014 | 0.009 | 0.012 | 0.005 | 0.008 | 0.007 | 0.011 | 0.007 |
| 3.0-3.2 | 0.006 | 0.007 | 0.011 | 0.005 | 0.010 | 0.009 | 0.005 | 0.006 | 0.008 | 0.008 | 0.008 | 0.004 |
| 3.2-3.4 | 0.004 | 0.008 | 0.008 | 0.010 | 0.012 | 0.008 | 0.008 | 0.009 | 0.010 | 0.007 | 0.007 | 0.005 |
| 3.4-3.6 | 0.006 | 0.007 | 0.011 | 0.006 | 0.011 | 0.010 | 0.014 | 0.012 | 0.008 | 0.005 | 0.007 | 0.006 |
| 3.6-3.8 | 0.005 | 0.007 | 0.007 | 0.007 | 0.006 | 0.010 | 0.005 | 0.003 | 0.007 | 0.005 | 0.008 | 0.006 |
| 3.8-4.0 | 0.006 | 0.009 | 0.009 | 0.007 | 0.003 | 0.002 | 0.004 | 0.007 | 0.009 | 0.010 | 0.005 | 0.004 |
| 4.0-4.2 | 0.003 | 0.007 | 0.005 | 0.006 | 0.012 | 0.010 | 0.006 | 0.005 | 0.008 | 0.007 | 0.008 | 0.002 |
| 4.2-4.4 | 0.006 | 0.004 | 0.001 | 0.007 | 0.008 | 0.012 | 0.012 | 0.010 | 0.005 | 0.008 | 0.009 | 0.005 |
| 4.4-4.6 | 0.005 | 0.007 | 0.010 | 0.007 | 0.010 | 0.008 | 0.007 | 0.008 | 0.014 | 0.008 | 0.008 | 0.009 |
| 4.6-4.8 | 0.007 | 0.009 | 0.003 | 0.006 | 0.009 | 0.012 | 0.012 | 0.004 | 0.007 | 0.011 | 0.003 | 0.002 |
| 4.8-5.0 | 0.010 | 0.006 | 0.005 | 0.005 | 0.008 | 0.006 | 0.004 | 0.006 | 0.005 | 0.006 | 0.008 | 0.004 |
| 5.0-5.2 | 0.005 | 0.003 | 0.007 | 0.010 | 0.012 | 0.014 | 0.009 | 0.007 | 0.007 | 0.007 | 0.007 | 0.009 |
| 5.2-5.4 | 0.005 | 0.009 | 0.006 | 0.006 | 0.007 | 0.006 | 0.006 | 0.004 | 0.004 | 0.007 | 0.006 | 0.009 |
| 5.4-5.6 | 0.003 | 0.007 | 0.005 | 0.004 | 0.006 | 0.002 | 0.005 | 0.006 | 0.008 | 0.004 | 0.003 | 0.002 |
| 5.6-5.8 | 0.006 | 0.004 | 0.004 | 0.004 | 0.008 | 0.007 | 0.006 | 0.010 | 0.006 | 0.007 | 0.007 | 0.002 |
| 5.8-6.0 | 0.005 | 0.004 | 0.009 | 0.003 | 0.011 | 0.007 | 0.007 | 0.006 | 0.007 | 0.007 | 0.012 | 0.006 |

TABLE XVII

DEGRADED ENERGY SPECTRUM OF TRANSMITTED PHOTONS AS FRACTION OF 6-$m_oc^2$
PHOTONS INCIDENT AT 30 DEG ON STRATIFIED SLABS
(EACH CASE HAD 1000 SAMPLE PHOTONS)

| Energy Interval $m_oc^2$ | 3 in. Polyethylene Lead Thickness (in.) | | | | 9 in. Polyethylene Lead Thickness (in.) | | | | 15 in. Polyethylene Lead Thickness (in.) | | | |
|---|---|---|---|---|---|---|---|---|---|---|---|---|
| | 0 | 0.1 | 0.3 | 0.5 | 0 | 0.1 | 0.3 | 0.5 | 0 | 0.1 | 0.3 | 0.5 |
| .1727-0.2 | 0.001 | 0 | 0 | 0 | 0.009 | 0 | 0 | 0 | 0.006 | 0 | 0 | 0 |
| 0.2-0.4 | 0.015 | 0 | 0 | 0 | 0.032 | 0 | 0 | 0 | 0.040 | 0 | 0 | 0 |
| 0.4-0.6 | 0.009 | 0.002 | 0.001 | 0 | 0.018 | 0.003 | 0 | 0.002 | 0.023 | 0 | 0.003 | 0.001 |
| 0.6-0.8 | 0.010 | 0.004 | 0.004 | 0.001 | 0.015 | 0.008 | 0.003 | 0.003 | 0.014 | 0.005 | 0.003 | 0.003 |
| 0.8-1.0 | 0.009 | 0.004 | 0.005 | 0.008 | 0.020 | 0.013 | 0.005 | 0.004 | 0.005 | 0.006 | 0.007 | 0.003 |
| 1.0-1.2 | 0.007 | 0.006 | 0.003 | 0.004 | 0.010 | 0.009 | 0.009 | 0.005 | 0.009 | 0.006 | 0.006 | 0.003 |
| 1.2-1.4 | 0.008 | 0.010 | 0.005 | 0.008 | 0.008 | 0.010 | 0.010 | 0.005 | 0.015 | 0.009 | 0.002 | 0.006 |
| 1.4-1.6 | 0.006 | 0.008 | 0.010 | 0.008 | 0.015 | 0.015 | 0.014 | 0.013 | 0.014 | 0.008 | 0.005 | 0.004 |
| 1.6-1.8 | 0.008 | 0.004 | 0.004 | 0.007 | 0.014 | 0.012 | 0.009 | 0.002 | 0.009 | 0.006 | 0.002 | 0.004 |
| 1.8-2.0 | 0.012 | 0.008 | 0.003 | 0.010 | 0.011 | 0.008 | 0.010 | 0.010 | 0.008 | 0.004 | 0.004 | 0.005 |
| 2.0-2.2 | 0.010 | 0.012 | 0.009 | 0.004 | 0.009 | 0.015 | 0.010 | 0.006 | 0.007 | 0.011 | 0.010 | 0.010 |
| 2.2-2.4 | 0.010 | 0.007 | 0.006 | 0.004 | 0.010 | 0.003 | 0.008 | 0.007 | 0.010 | 0.005 | 0.001 | 0.006 |
| 2.4-2.6 | 0.007 | 0.005 | 0.010 | 0.009 | 0.007 | 0.008 | 0.006 | 0.007 | 0.002 | 0.009 | 0.011 | 0.005 |
| 2.6-2.8 | 0.005 | 0.009 | 0.005 | 0.010 | 0.009 | 0.005 | 0.005 | 0.003 | 0.004 | 0.009 | 0.005 | 0.005 |
| 2.8-3.0 | 0.011 | 0.008 | 0.008 | 0.009 | 0.017 | 0.012 | 0.009 | 0.008 | 0.009 | 0.009 | 0.006 | 0.006 |
| 3.0-3.2 | 0.004 | 0.009 | 0.010 | 0.009 | 0.010 | 0.009 | 0.008 | 0.004 | 0.008 | 0.008 | 0.005 | 0.003 |
| 3.2-3.4 | 0.002 | 0.008 | 0.007 | 0.012 | 0.006 | 0.007 | 0.006 | 0.002 | 0.010 | 0.010 | 0.007 | 0.007 |
| 3.4-3.6 | 0.005 | 0.007 | 0.006 | 0.009 | 0.007 | 0.008 | 0.009 | 0.012 | 0.010 | 0.011 | 0.007 | 0.009 |
| 3.6-3.8 | 0.006 | 0.007 | 0.012 | 0.009 | 0.011 | 0.011 | 0.005 | 0.002 | 0.009 | 0.009 | 0.008 | 0.006 |
| 3.8-4.0 | 0.006 | 0.008 | 0.006 | 0.006 | 0.005 | 0.011 | 0.005 | 0.004 | 0.012 | 0.010 | 0.006 | 0.005 |
| 4.0-4.2 | 0.003 | 0.006 | 0.008 | 0.007 | 0.011 | 0.011 | 0.002 | 0.004 | 0.008 | 0.008 | 0.010 | 0.008 |
| 4.2-4.4 | 0.007 | 0.005 | 0.007 | 0.005 | 0.006 | 0.012 | 0.010 | 0.009 | 0.007 | 0.013 | 0.005 | 0.003 |
| 4.4-4.6 | 0.006 | 0.003 | 0.005 | 0.007 | 0.010 | 0.007 | 0.007 | 0.008 | 0.009 | 0.003 | 0.006 | 0.004 |
| 4.6-4.8 | 0.008 | 0.003 | 0.008 | 0.009 | 0.010 | 0.008 | 0.007 | 0.006 | 0.003 | 0.007 | 0.003 | 0.004 |
| 4.8-5.0 | 0.011 | 0.005 | 0.003 | 0.004 | 0.011 | 0.010 | 0.014 | 0.004 | 0.010 | 0.010 | 0.006 | 0.007 |
| 5.0-5.2 | 0.005 | 0.011 | 0.007 | 0.011 | 0.014 | 0.005 | 0.006 | 0.005 | 0.008 | 0.004 | 0.009 | 0.005 |
| 5.2-5.4 | 0.004 | 0.009 | 0.009 | 0.006 | 0.005 | 0.008 | 0.005 | 0.003 | 0.002 | 0.002 | 0.001 | 0.004 |
| 5.4-5.6 | 0.003 | 0.007 | 0.010 | 0.007 | 0.005 | 0.007 | 0.003 | 0.006 | 0.009 | 0.009 | 0.007 | 0.003 |
| 5.6-5.8 | 0.005 | 0.005 | 0.006 | 0.005 | 0.008 | 0.007 | 0.007 | 0.006 | 0.005 | 0.004 | 0.002 | 0.001 |
| 5.8-6.0 | 0.005 | 0.005 | 0.004 | 0.004 | 0.011 | 0.007 | 0.005 | 0.003 | 0.007 | 0.004 | 0.007 | 0.009 |

TABLE XVIII

DEGRADED ENERGY SPECTRUM OF TRANSMITTED PHOTONS AS FRACTION OF 6-$m_oc^2$ PHOTONS INCIDENT AT 60 DEG ON STRATIFIED SLABS (EACH CASE HAD 1000 SAMPLE PHOTONS)

| Energy Interval $m_oc^2$ | 3 in. Polyethylene Lead Thickness (in.) | | | | 9 in. Polyethylene Lead Thickness (in.) | | | | 15 in. Polyethylene Lead Thickness (in.) | | | |
|---|---|---|---|---|---|---|---|---|---|---|---|---|
| | 0 | 0.1 | 0.3 | 0.5 | 0 | 0.1 | 0.3 | 0.5 | 0 | 0.1 | 0.3 | 0.5 |
| .1727-0.2 | 0.002 | 0 | 0 | 0 | 0.011 | 0 | 0 | 0 | 0.007 | 0 | 0 | 0 |
| 0.2-0.4 | 0.032 | 0.003 | 0 | 0 | 0.045 | 0.001 | 0 | 0 | 0.040 | 0 | 0.001 | 0 |
| 0.4-0.6 | 0.011 | 0.005 | 0.002 | 0.003 | 0.035 | 0.009 | 0.001 | 0.002 | 0.024 | 0.004 | 0 | 0 |
| 0.6-0.8 | 0.024 | 0.006 | 0.009 | 0.003 | 0.024 | 0.019 | 0.006 | 0.005 | 0.008 | 0.008 | 0.002 | 0 |
| 0.8-1.0 | 0.015 | 0.016 | 0.010 | 0.005 | 0.026 | 0.012 | 0.006 | 0.004 | 0.016 | 0.007 | 0.003 | 0 |
| 1.0-1.2 | 0.014 | 0.008 | 0.009 | 0.005 | 0.015 | 0.012 | 0.008 | 0.007 | 0.018 | 0.009 | 0.004 | 0.005 |
| 1.2-1.4 | 0.005 | 0.014 | 0.013 | 0.008 | 0.014 | 0.009 | 0.006 | 0.005 | 0.003 | 0.011 | 0.007 | 0.002 |
| 1.4-1.6 | 0.014 | 0.010 | 0.008 | 0.005 | 0.011 | 0.010 | 0.005 | 0.007 | 0.008 | 0.010 | 0.003 | 0.005 |
| 1.6-1.8 | 0.009 | 0.008 | 0.006 | 0.004 | 0.015 | 0.007 | 0.008 | 0.011 | 0.003 | 0.006 | 0.006 | 0.004 |
| 1.8-2.0 | 0.008 | 0.011 | 0.010 | 0.005 | 0.006 | 0.008 | 0.009 | 0.007 | 0.006 | 0.009 | 0.005 | 0.002 |
| 2.0-2.2 | 0.010 | 0.004 | 0.012 | 0.008 | 0.007 | 0.013 | 0.008 | 0.006 | 0.010 | 0.004 | 0.006 | 0.002 |
| 2.2-2.4 | 0.011 | 0.007 | 0.002 | 0.007 | 0.008 | 0.006 | 0.002 | 0.003 | 0.005 | 0.008 | 0.003 | 0.002 |
| 2.4-2.6 | 0.012 | 0.014 | 0.014 | 0.011 | 0.007 | 0.008 | 0.003 | 0.005 | 0.002 | 0.003 | 0.004 | 0.003 |
| 2.6-2.8 | 0.004 | 0.007 | 0.002 | 0.003 | 0.006 | 0.006 | 0.005 | 0.004 | 0.002 | 0.004 | 0.003 | 0.003 |
| 2.8-3.0 | 0.011 | 0.007 | 0.007 | 0.007 | 0.011 | 0.010 | 0.012 | 0.007 | 0.007 | 0.007 | 0.001 | 0.002 |
| 3.0-3.2 | 0.005 | 0.008 | 0.002 | 0.003 | 0.009 | 0.005 | 0.005 | 0.002 | 0.004 | 0.004 | 0.006 | 0.003 |
| 3.2-3.4 | 0.007 | 0.005 | 0.008 | 0.006 | 0.005 | 0.006 | 0.005 | 0.003 | 0.006 | 0.002 | 0.003 | 0.002 |
| 3.4-3.6 | 0.007 | 0.007 | 0.007 | 0.007 | 0.005 | 0.008 | 0.004 | 0.005 | 0.004 | 0.007 | 0.005 | 0.006 |
| 3.6-3.8 | 0.008 | 0.004 | 0.003 | 0.004 | 0.006 | 0.010 | 0.004 | 0.004 | 0.005 | 0.001 | 0.001 | 0 |
| 3.8-4.0 | 0.003 | 0.008 | 0.003 | 0.006 | 0.006 | 0.005 | 0.004 | 0.003 | 0.003 | 0.005 | 0.001 | 0.002 |
| 4.0-4.2 | 0.005 | 0.006 | 0.008 | 0.009 | 0.006 | 0.011 | 0.008 | 0.004 | 0.006 | 0.005 | 0.002 | 0.001 |
| 4.2-4.4 | 0.010 | 0.009 | 0.007 | 0.005 | 0.005 | 0.007 | 0.005 | 0.003 | 0.002 | 0.001 | 0.001 | 0.003 |
| 4.4-4.6 | 0.007 | 0.005 | 0.003 | 0.002 | 0.006 | 0.003 | 0.002 | 0.002 | 0.005 | 0 | 0.003 | 0.002 |
| 4.6-4.8 | 0.010 | 0.013 | 0.007 | 0.006 | 0.007 | 0.005 | 0.002 | 0 | 0.002 | 0.001 | 0.002 | 0.004 |
| 4.8-5.0 | 0.012 | 0.010 | 0.009 | 0.006 | 0.007 | 0.007 | 0.003 | 0.002 | 0.001 | 0.004 | 0.003 | 0.001 |
| 5.0-5.2 | 0.009 | 0.008 | 0.011 | 0.005 | 0.010 | 0.007 | 0.004 | 0.002 | 0.003 | 0.003 | 0.003 | 0.002 |
| 5.2-5.4 | 0.008 | 0.006 | 0.007 | 0.007 | 0.007 | 0.006 | 0.006 | 0.004 | 0.002 | 0.003 | 0.001 | 0.001 |
| 5.4-5.6 | 0.006 | 0.009 | 0.005 | 0.002 | 0.006 | 0.005 | 0.001 | 0.002 | 0.002 | 0.004 | 0 | 0 |
| 5.6-5.8 | 0.005 | 0.003 | 0.005 | 0.005 | 0.006 | 0.004 | 0.003 | 0.003 | 0.001 | 0 | 0.001 | 0.001 |
| 5.8-6.0 | 0.006 | 0.008 | 0.002 | 0.002 | 0.009 | 0.002 | 0.004 | 0.001 | 0.002 | 0.003 | 0.001 | 0 |

N = the number of sample source photons,

$\delta$ = the standard deviation.

Having the standard deviation, it is possible to find a confidence interval such that the true value of the fraction F will lie within the limits of the interval about F with a given probability. This is expressed mathematically for the 95 per cent confidence interval as[41]

$$P\left[F - 1.96\delta < \tilde{F} < F + 1.96\delta\right] \cong 0.95 \tag{40}$$

and for the 50 per cent confidence interval as

$$P\left[F - 0.6745\delta < \tilde{F} < F + 0.6745\delta\right] \cong 0.5 \tag{41}$$

The estimated variance of the energy fractions could be computed as a part of the calculation. This was not done, however, because of space limitations in the memory of the ORACLE, and because some experimental data was available for evaluation of errors.

## Comparison of Results with Experiment and Other Calculations

The values given in Table VI for the fraction of energy transmitted through lead slabs was directly comparable to results of calculation by Peebles.[42] His values were obtained using the multiple scattering method discussed in Chapter I. His data for lead slabs were expected to be

---

[41] A. M. Mood, op. cit., pg. 236.

[42] G. H. Peebles, Gamma-Ray Transmission Through Finite Slabs, (Rand Corporation Report), report number R-240 (1952).

accurate since photons scattered more than three times contribute little to the energy transmitted, and his extrapolation to account for the contribution of those scattered more than three times could not introduce an appreciable error even if it was off to some extent. There was a slight difference in the source energy used in the two calculations which should introduce a small difference in comparing the data: Peebles' data was for a source energy of $2.5\text{-}m_0c^2$ whereas the values taken from Table VI were for a source energy of $2.45\text{-}m_0c^2$. Figure 5 shows the comparison of the two calculations where the source radiation was normally incident on the slabs. Peebles' data was taken from a graph where errors as large as 5 per cent could be made in reading values in some regions. The values from this calculation correspond very well with those obtained by Peebles. The one value from this calculation located at 4.89 mean free paths (m.f.p.) appears to be out of line with the others as is likely for some values obtained with this type of statistical estimate. A smooth curve through the results of this calculation, ignoring the value at 4.89 m. f. p., would be approximately 8% above Peebles' value at 5 m. f. p. Figure 6 gives the the values from Peebles' calculation in comparison with values taken from Table VI for the source radiation incident at 60 deg on lead slabs. There is very good agreement for all values out to 3.26 m. f. p. The one value at 6.52 m. f. p. differs to some extent from the value obtained by Peebles; however, it appears to be out of line with a smooth curve through the other values so the error could again be attributed to statistics. A comparison of the calculated fraction of photons transmitted through lead slabs is given in Fig. 7 for cases corresponding to those presented in Figs. 5 and 6. All values obtained

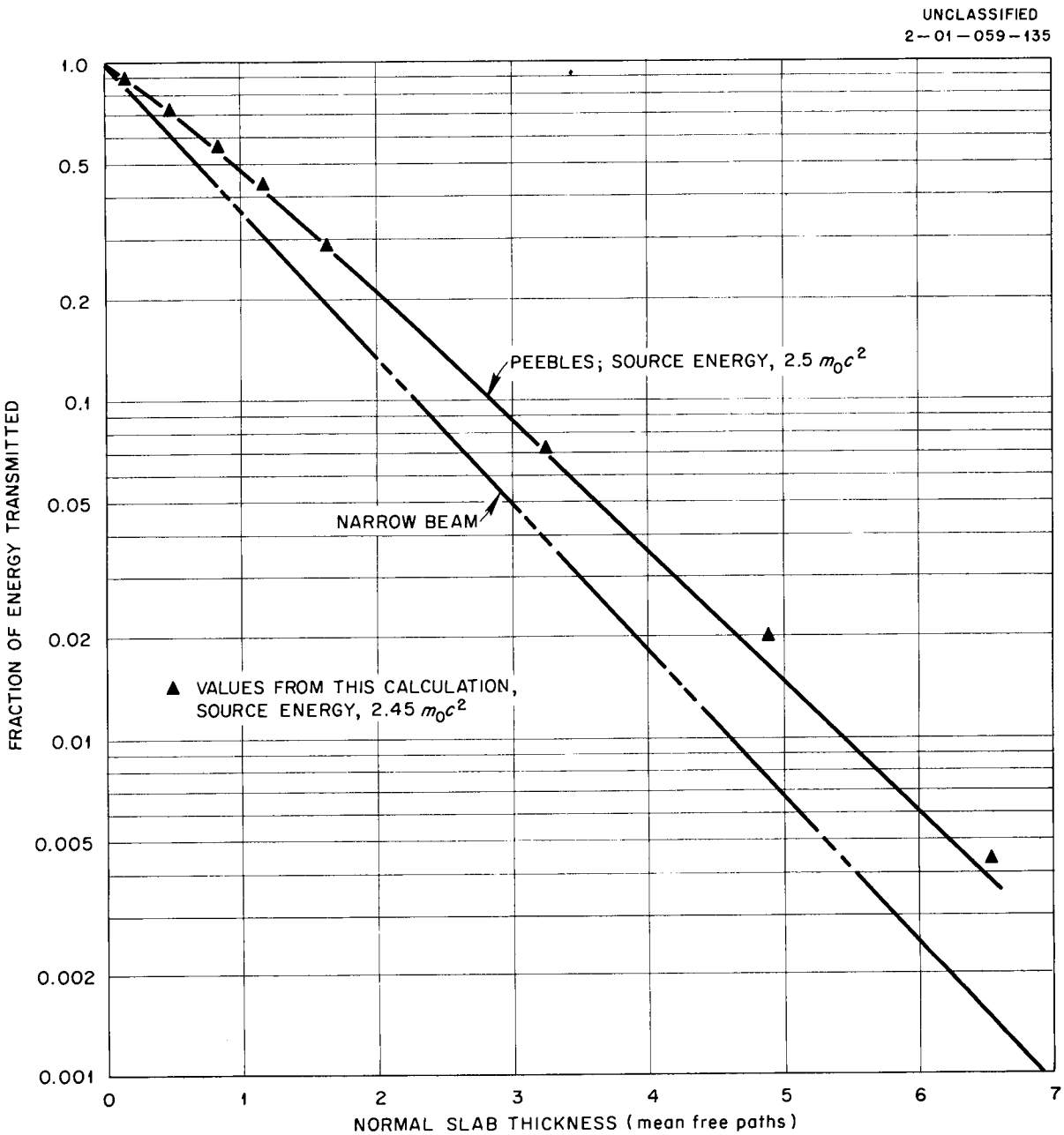


Fig. 5. Comparison of Calculated Values of Fraction of Energy of Gamma Radiation Incident at 0 deg that is Transmitted Through Lead Slabs.

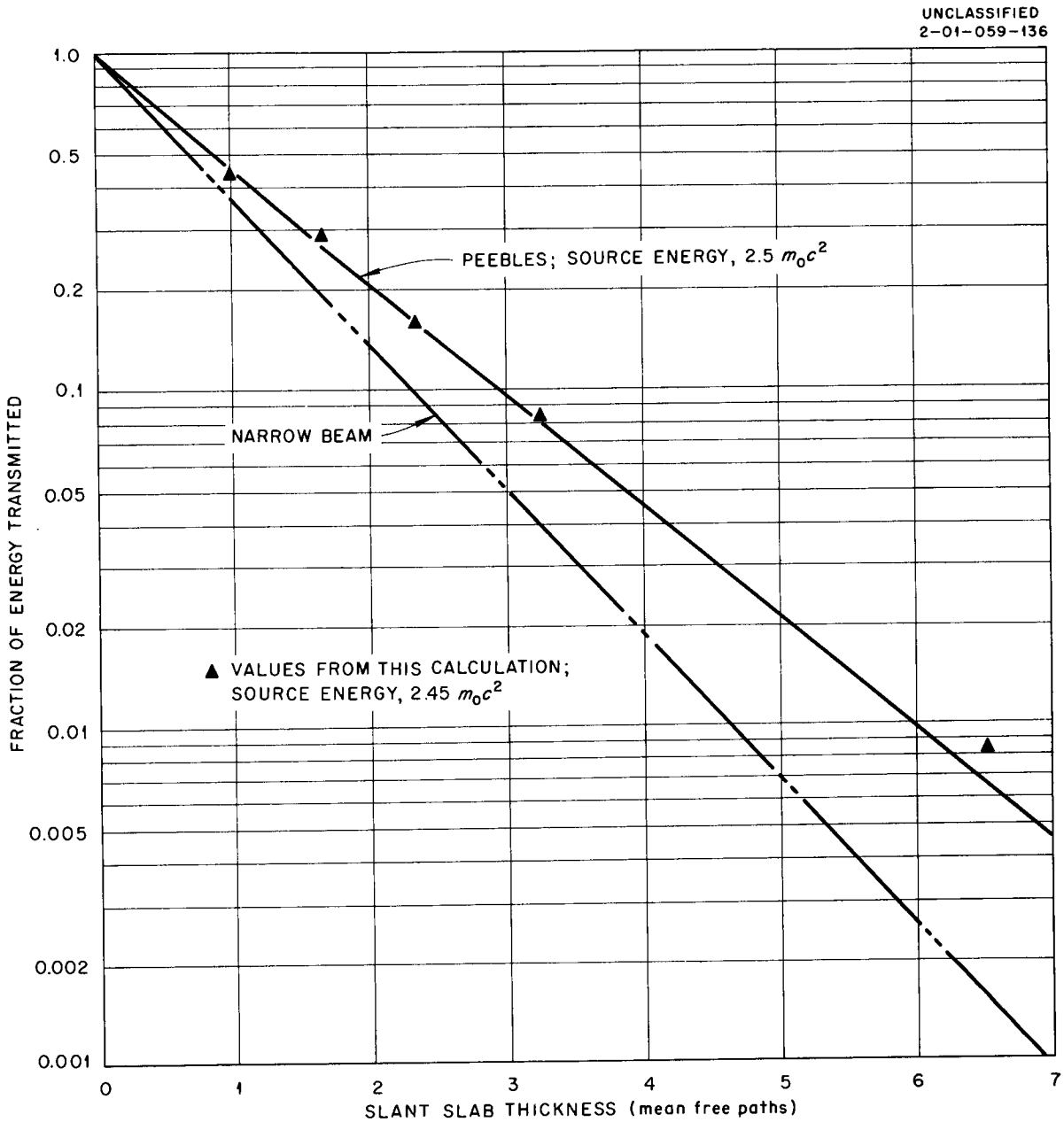


Fig. 6. Comparison of Calculated Values of the Fraction of Energy of Gamma Radiation Incident at 60 deg that is Transmitted Through Lead Slabs.

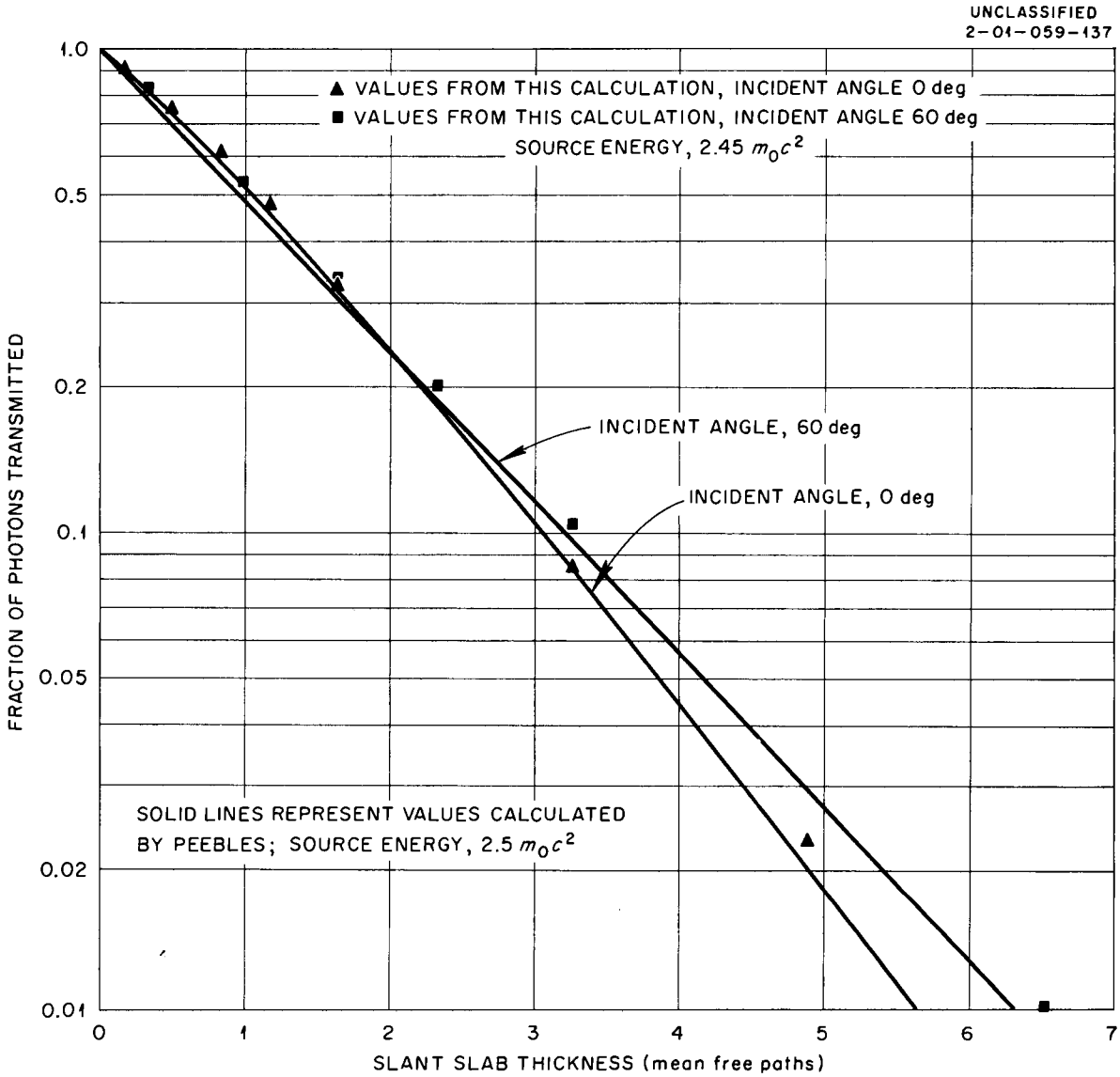


Fig. 7. Comparison of Calculated Values of the Fraction of Slant Incident Source Photons Transmitted Through Lead Slabs.

except for the one for an incident angle of 0 deg at 4.89 m. f. p. are within 10 per cent of Peebles' values. In general, there seems to be better agreement for the cases corresponding to an incident angle of 0 deg. The one value in Fig. 7 at 4.89 m. f. p. is for the same case from which the spurious value in Fig. 5 was obtained.

Kahn[43] and Peebles have calculated the fraction of energy from a 2.5-$m_oc^2$ source transmitted through slabs of a pure Compton scatterer. In both calculations the radiation was normally incident on the slabs where the geometry was the same as used in this calculation. Peebles carried his calculation to a very low photon energy although he does not indicate the exact value of the cut off energy. His method of calculation was somewhat different from that previously discussed and is difficult to evaluate quantitatively.[44] Kahn carried his calculation to a cut off energy of 0.1-$m_oc^2$. The results given in Table VIII are comparable with Kahn's and Peebles'; however, a cut off energy of 0.1727-$m_oc^2$ was used. The results of the three calculations are given in Fig. 8. Peebles had previously made a comparison of his calculation with that of Kahn's at 4 m. f. p.[45] He was able to account for the difference within 2 per cent because of the difference in cut off energy. Kahn's value differs from Peebles' by 21 per cent at 4 m. f. p., and the interpolated value from this calculation is 37 per cent below that obtained by Peebles at the same point because of the higher cut off energy of

---

[43]H. Kahn, Nucleonics, Part II, 6, 60 (June, 1950).

[44]G. H. Peebles, op. cit., pg. 81-84.

[45]G. H. Peebles, op. cit., pg. 174.

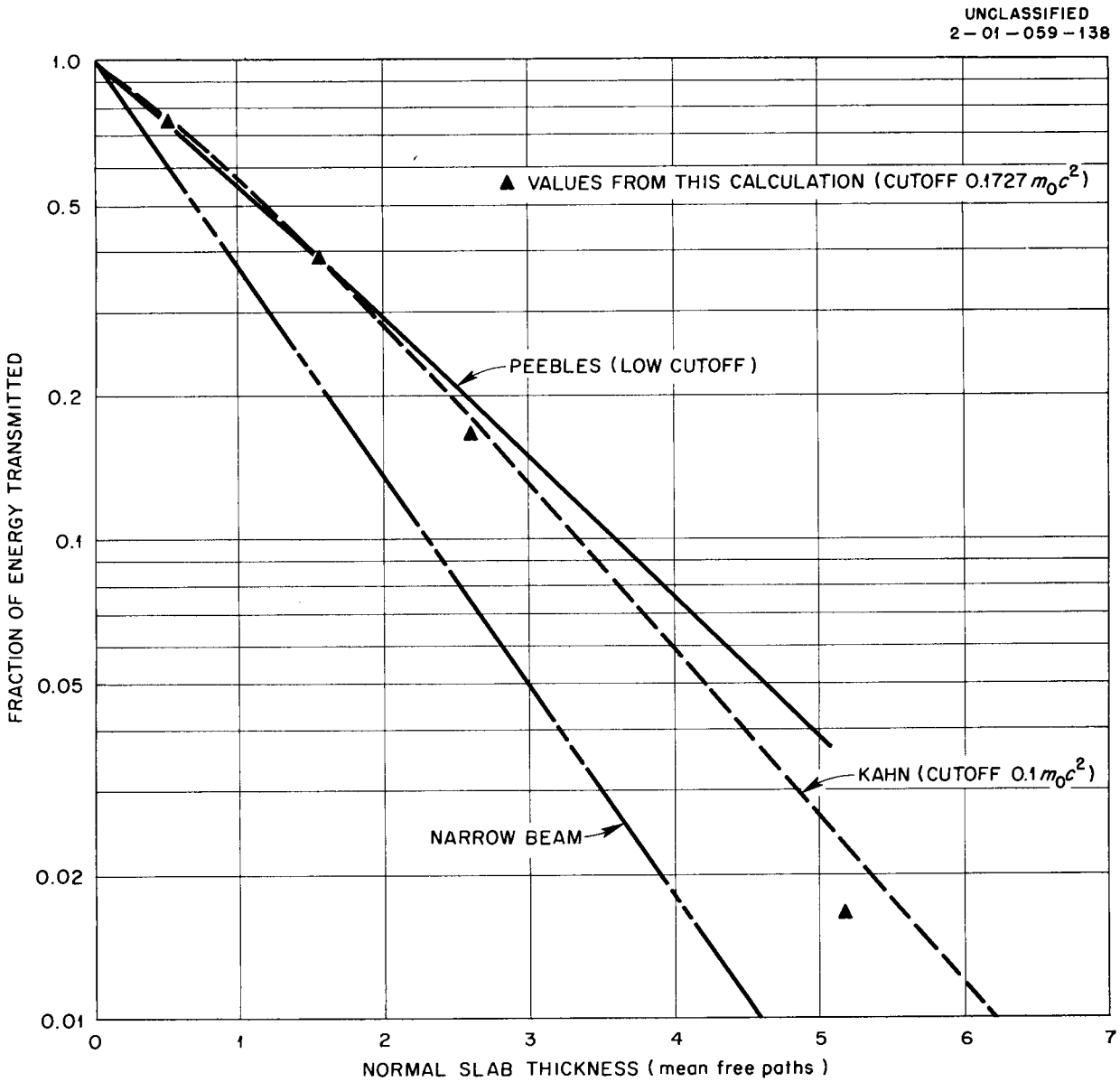


Fig. 8. Comparison of Calculated Values of the Fraction of Energy of Gamma Radiation Incident at 0 deg that is Transmitted Through Slabs Composed of a Pure Compton Scatterer.

$0.1727\text{-}m_0c^2$. The curve through Peebles' data has a decidedly different shape from that obtained in this calculation or that obtained in Kahn's calculation; however, they are all very close to the same values for a slab with thickness of less than 2 m. f. p. The cut off energy makes little difference in the values obtained for the thin slabs because the source radiation will not make a sufficient number of collisions on the average to build up the low energy part of the spectra. The two values obtained in this calculation for slabs with thicknesses less than 2 m. f. p. fall on the values obtained by Kahn with no detectable difference.

The fraction of energy transmitted through the slabs obtained in this calculation can be defined in more detail as the ratio of the energy penetrating the slab per unit surface area to the energy incident on the slab per unit surface area. As the values stand they are not directly comparable with experimental values such as those obtained by Kirn, Kennedy, and Wyckoff.[46] They obtained the ratio of the response of an ionization chamber placed on the side of the slab opposite the source to the response when the slab was removed. In what follows, this ratio will be termed the fraction of detector response. In general, the fraction of detector response is not the fraction of energy transmitted, in fact, there is a considerable difference for larger angles of incidence of the source radiation. The difference can be accounted for qualitatively by noting that the projected area on the surface of the slab of a spherical detector varies

---

[46] F. S. Kirn, R. J. Kennedy, and H. O. Wyckoff, Radiology, 63, 94 (July, 1954).

with the angle of projection. The result is that the radiation energy transmitted at large angles with respect to the slab normal per unit area of slab surface will give rise to a greater detector response than the same amount of energy transmitted along the normal per unit area of surface.

To obtain the fraction of detector response additional data from the calculation was used in the manner described in Appendix A. The calculated values plotted in Figs. 9, 10, and 11 were obtained in this way. The calculated values are for an infinitesimal spherical detector and will differ by a small percentage from those obtained in experiment. In addition, since this calculation involved some graphical approximation, the values may be in error by as much as 10 per cent for the thick slabs.

Kirn, Kennedy, and Wyckoff obtained the fraction of detector response for lead slabs and stratified slabs where the radiation was emitted from a $Co^{60}$ or a $Cs^{137}$ source. The experimental arrangement was such that the data obtained applied to the same geometrical arrangement as used in this calculation. Although the density of the lead used in the experiment was not given, it was assumed to be 11.3 which is the same as used in this calculation. Figure 9 presents a comparison of the experimental values with those obtained in this calculation and with those obtained in the calculation by Berger and Doggett.[47] The data attributed to the latter calculation were the result of interpolation and could be slightly in error. The four values from this calculation correspond to the values at the same slab

---

[47] M. J. Berger and J. Doggett, loc. cit.

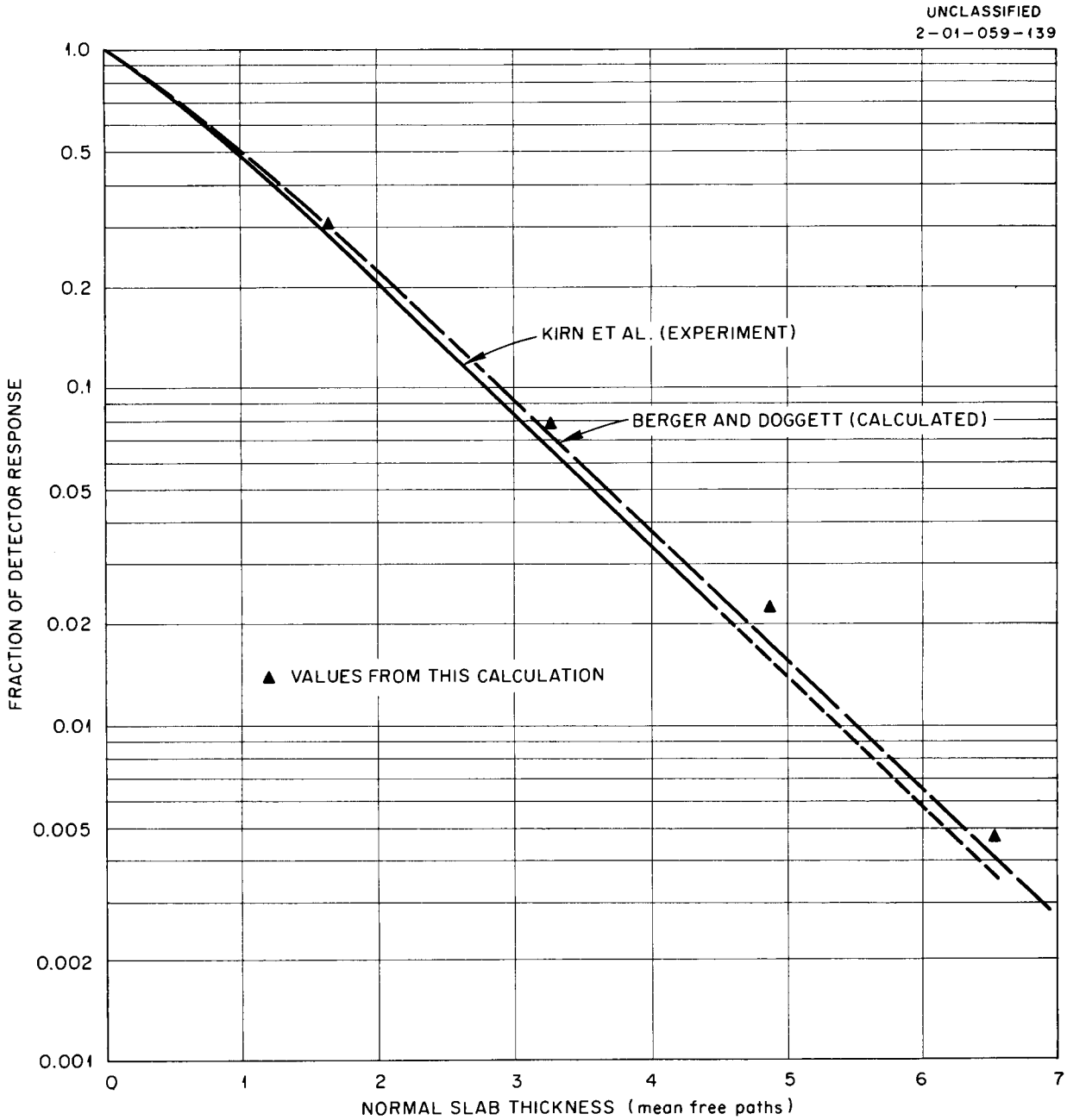


Fig. 9. Comparison of Calculated and Experimental Values of the Fraction of Detector Response for the Case of $Co^{60}$ Source Photons Incident at 0 deg on a Lead Slab.

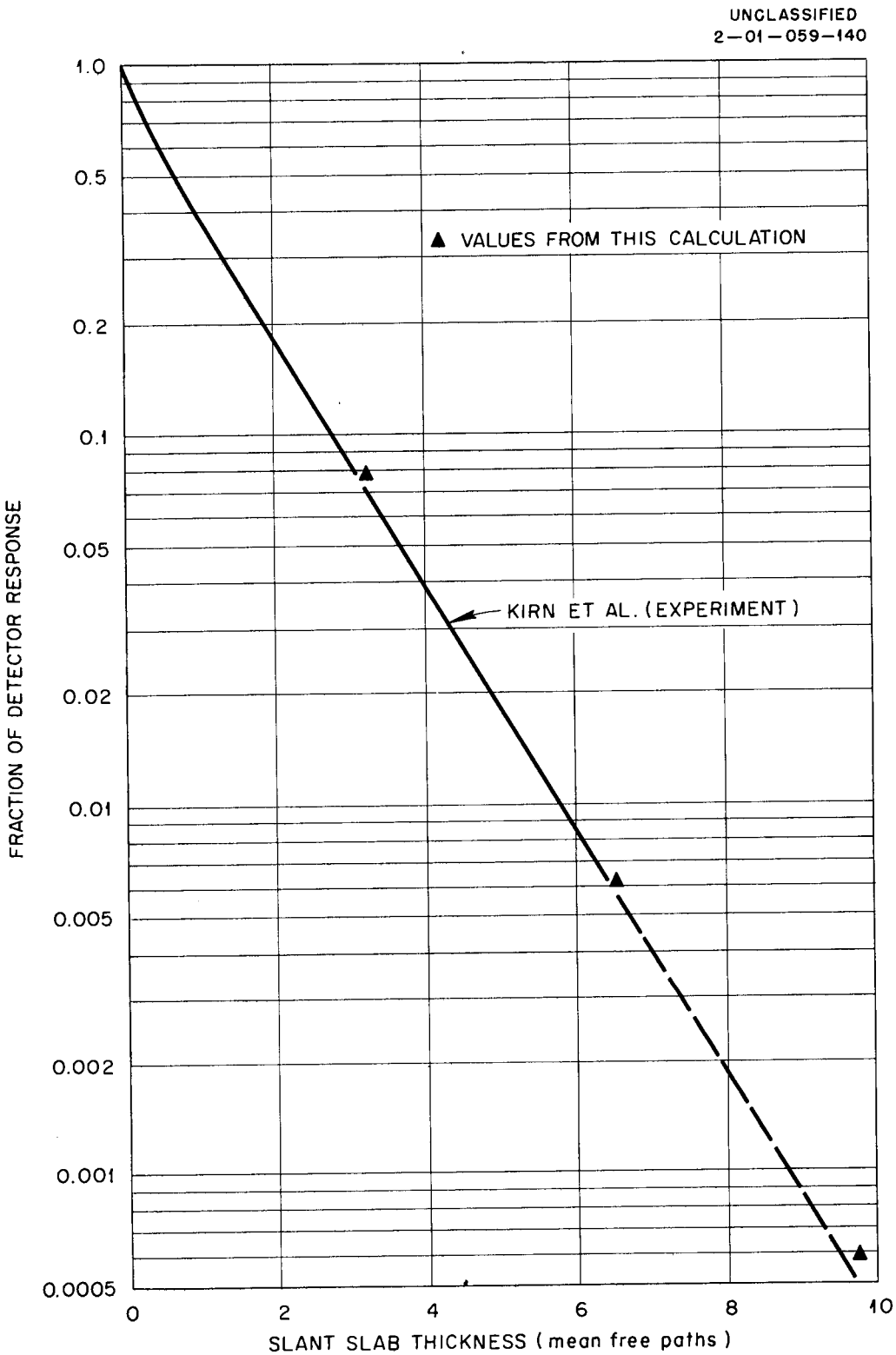


Fig. 10. Comparison of Calculated and Experimental Values of the Fraction of Detector Response for the Case of $Co^{60}$ Source Photons Incident at 60 deg on a Lead Slab.

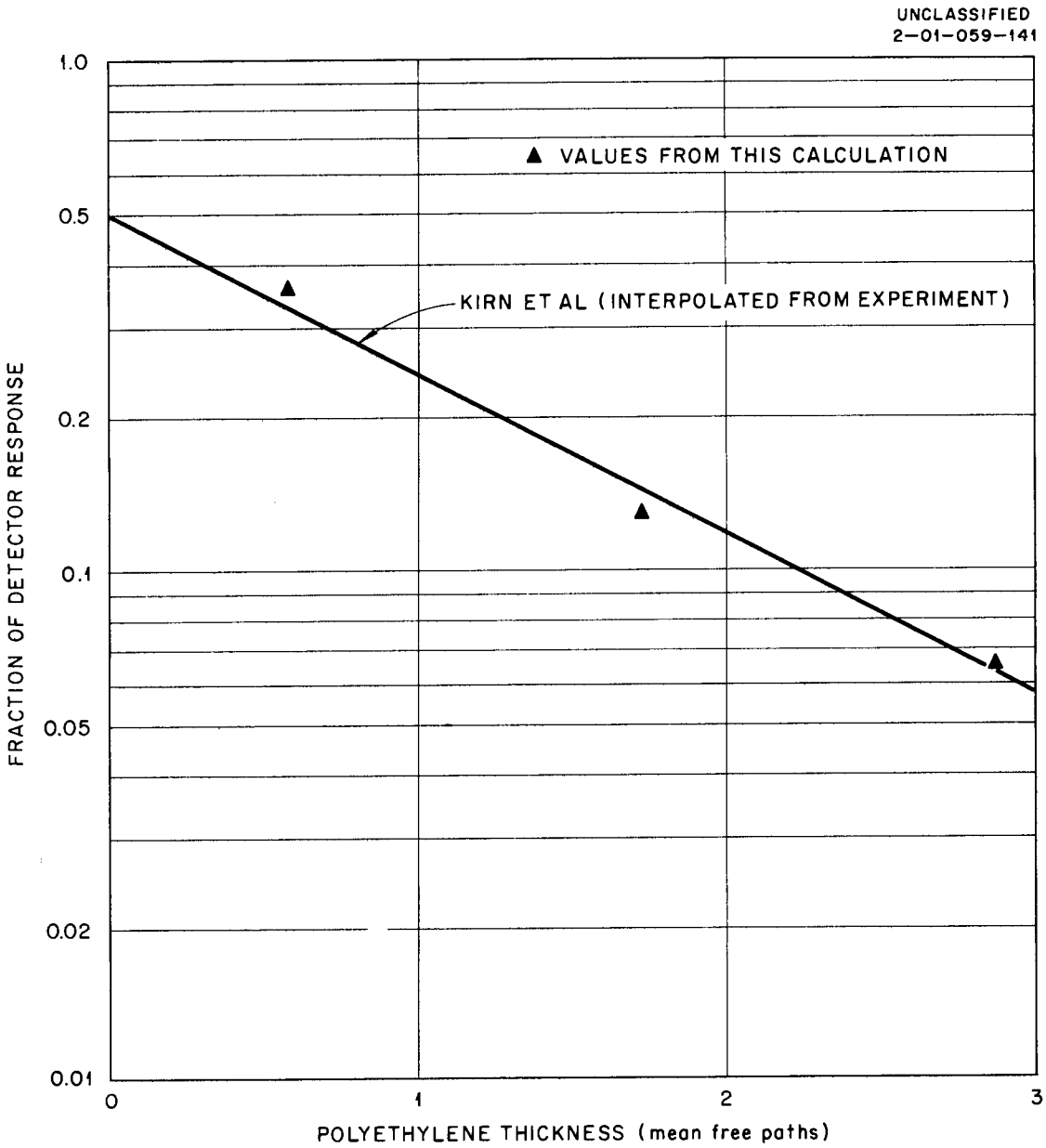


Fig. 11. Comparison of Calculated and Experimental Values of the Fraction of Detector Response for the Case of 2.00-$m_0c^2$ Photons Incident at 0 deg on a Stratified Slab of Polyethylene Followed by 0.5 in. of Lead.

thicknesses given in Fig. 5. A smooth curve through the points, ignoring the one at 4.89 m. f. p. as before, gives a value approximately 15 per cent high at 5 m. f. p. slab thickness while the value obtained by Berger and Doggett is approximately 7 per cent high at the same thickness. The differences are less for the thinner slabs in both calculations.

In Fig. 10 three values from this calculation are compared with experiment where the $Co^{60}$ source radiation was incident at 60 deg. Again the calculated values are high.

A likely explanation for the calculated data being, in general, high in comparison with experiment is the inaccuracy of the cross section data used in the calculations. In addition, however, all calculations ignored the coherent scattering and used the angular distribution of incoherent scattering from free electrons. Both of these oversights to simplify the calculations tend to increase the scattering in the forward direction, and as discussed in Chapter III, could account for some of the difference particularly for slabs composed of a heavy element such as lead.

In Fig. 11 a comparison of experimental and calculated values is presented for the fraction of detector response where the source energy was $2.0\text{-}m_oc^2$ and the radiation was normally incident on stratified slabs. The experimental values attributed to Kirn, Kennedy, and Whckoff were interpolated from results of their experiments and could be in error by as much as 10 per cent. All the calculated values are within 10 per cent of the curve through their data.

## Discussion of Stratified Slab Data

The high cut off energy of $0.1727\text{-}m_oc^2$ will not affect the values obtained for the fraction of energy transmitted through the stratified slabs where lead follows polyethylene because of the small probability that photons of that energy or below will penetrate the lead. The values for the fraction of energy transmitted given in Tables IX through XII are plotted in Figs. 12 and 13. The solid lines were not extended to the points for zero thickness of lead because the cut off energy would make these values lower than the true values. It will be noted that the lines are straight and would extend through the points at zero lead thickness. This can be accounted for because all the values represent the fraction of energy transmitted between $0.1727\text{-}m_oc^2$ and the source energy; however, for a finite thickness of lead following the polyethylene there is essentially no contribution to the energy transmitted below $0.1727\text{-}m_oc^2$. The curves plotted in Figs. 12 and 13 are estimated to have an error of less than 10 per cent. The change in energy spectrum of transmitted photons through a typical stratified slab is shown in Fig. 14. The values for Fig. 14 were obtained from Table XVI.

Methods to derive the energy and photon distribution for other than monodirectional sources are given in Appendix B.

UNCLASSIFIED
2-01-059-10

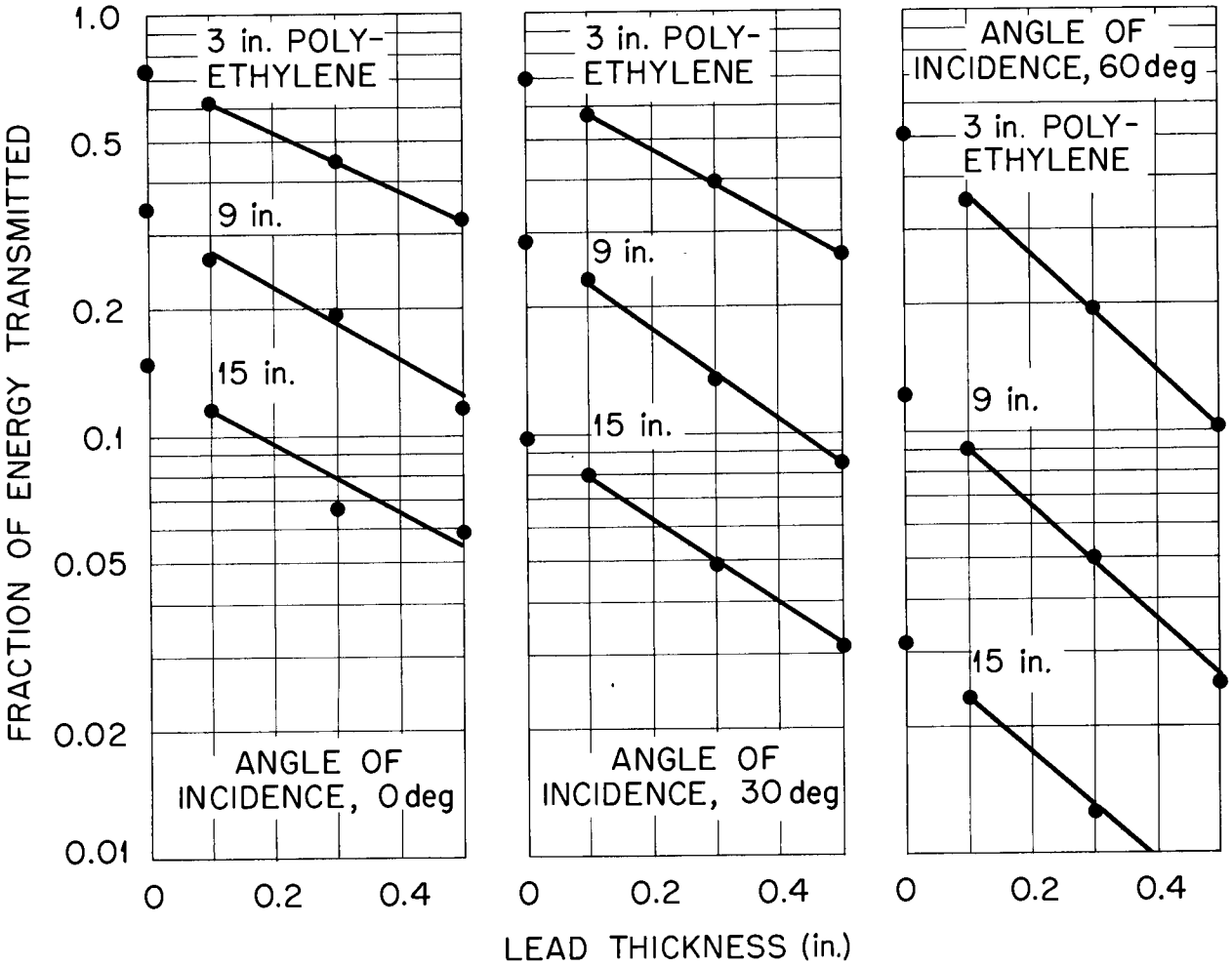


Fig. 12. Fraction of Energy of Slant Incident 2-$m_0c^2$ Photons that is Transmitted Through Stratified Slabs of Polyethylene Backed by Lead.

UNCLASSIFIED
2-01-059-9

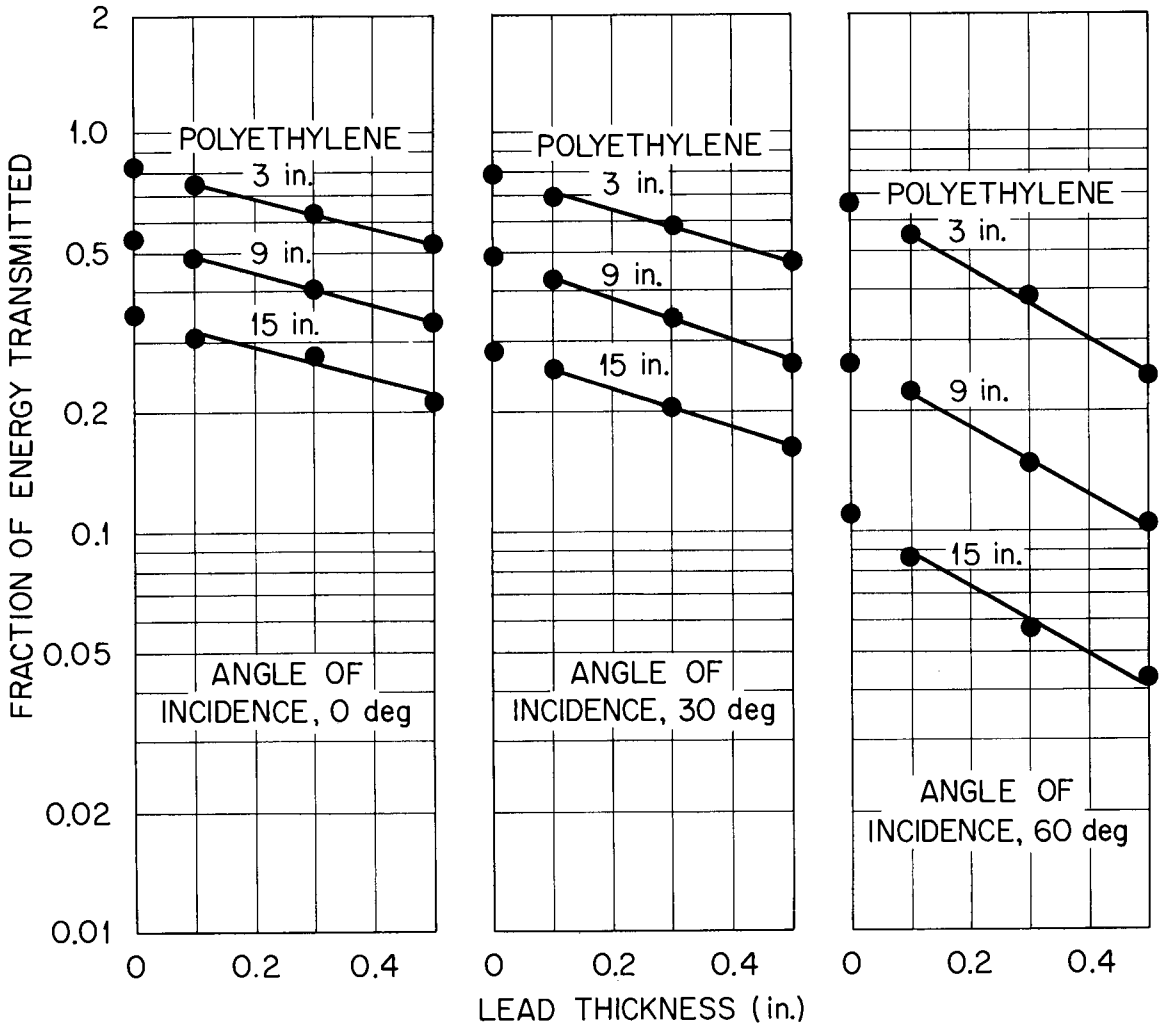


Fig. 13. Fraction of Energy of Slant Incident 6-$m_0c^2$ Photons that is Transmitted Through Stratified Slabs of Polyethylene Backed by Lead.

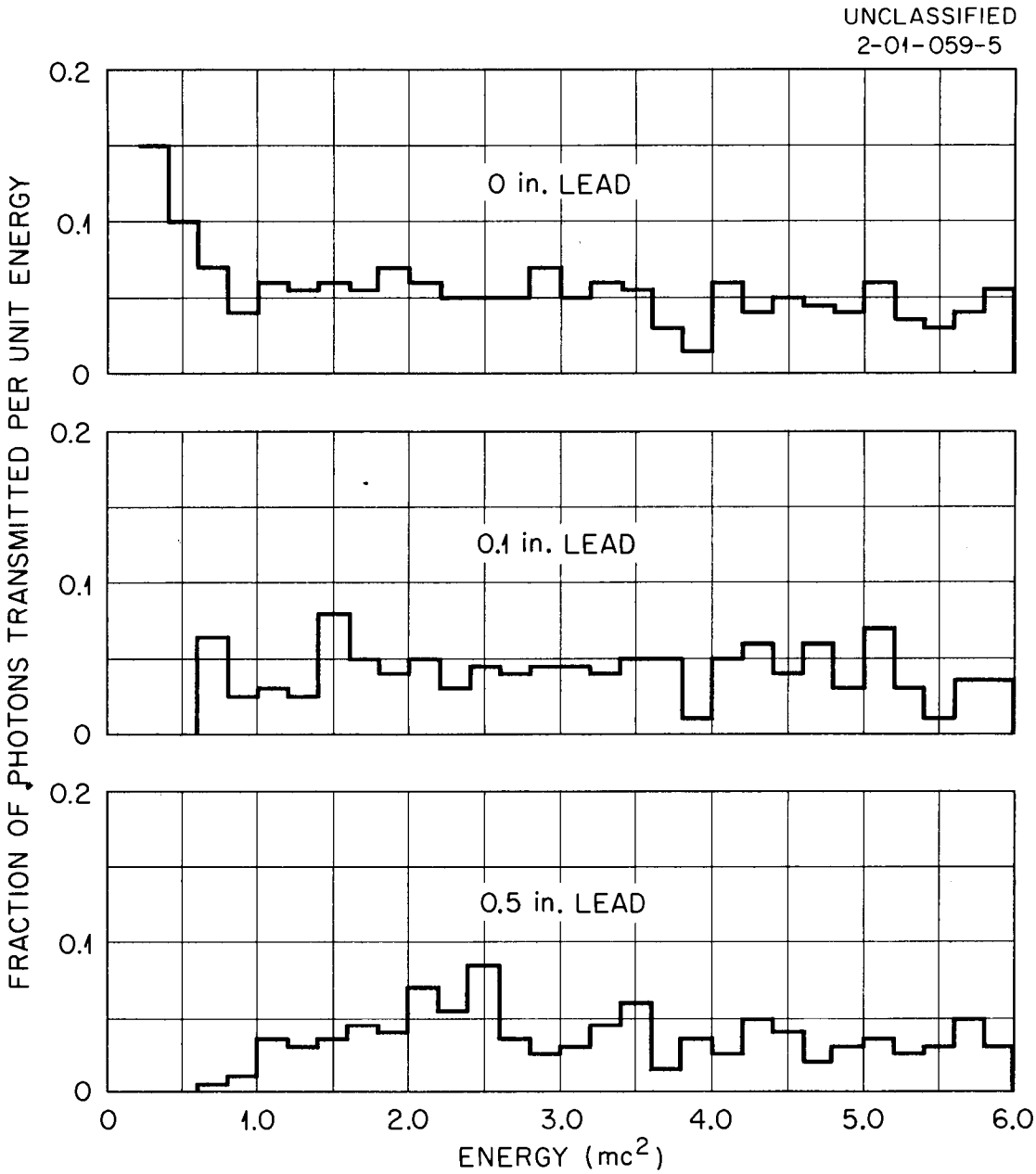


Fig. 14. Energy Spectrum Resulting from Degraded Normally Incident 6-$m_0c^2$ Photons Transmitted Through Stratified Slab of 9 in. of Polyethylene Backed by Lead.

# BIBLIOGRAPHY

# BIBLIOGRAPHY


Bethe, H. A. and Ashkin, J., "Penetration of Gamma Rays," Vol. 1, Part II-3 of Experimental Nuclear Physics, E. Segre, Ed., (John Wiley and Sons, Inc., New York, 1953).

Berger, M. J. and Doggett, J., Reflection and Transmission of $\gamma$-Radiation by Barriers: Semi-Analytic Monte Carlo Calculation, to be published.

Bethe, Fano, and Karr, Part I, Phys. Rev. 76, 538 (1949).

Compton, A. H. and Allison, S. K., X-Rays in Theory and Experiment, (D. Van Nostrand Company, Inc., New York, 1953).

Fano, U., Part II, Phys. Rev. 76, 739 (1949).

Fano, U., Part I, Nucleonics 11, 8 (Aug. 1953).

Fano, U., "Gamma Ray Attenuation," Vol. 1, Chap. 2.3, Reactor Handbook (USAEC Technical Information Service report), report number AECD-3645 (1955).

Foldy, L. L., Part I, Phys. Rev. 81 395 (1951).

Foldy, L. L., Part III, Phys. Rev. 82, 927 (1951).

Foldy, L. L. and Osborn, R. K., Part II, Phys. Rev. 81, 400 (1951).

Goldstein, H., Estimates of the Effect of Fluorescence and Annihilation Radiation on Gamma Ray Penetration, (Nuclear Development Associates report), report number NDA 15C-31 (1954).

Goldstein, H., and Aronson, R., Status Report on Calculations of Gamma Ray Penetration, (Nuclear Development Associates report), report number NYO-3079 (1953).

Goldstein, H., and Wilkins, J. E., Calculations of the Penetration of Gamma Rays, (USAEC Technical Information Service report), report number NYO-3075 (1954).

Heitler, W., The Quantum Theory of Radiation, (Oxford Press, 1954).

Householder, A. S., Principles of Numerical Analysis, (McGraw-Hill Book Company, New York, 1953).

Kahn, H., Nucleonics, Part I, 6, 27 (May 1950).

Kahn, H., Nucleonics, Part II, 6, 60 (June 1950).

Karr, P. R., and Lankin, J. C., Part III, Phys. Rev. 76, 1843 (1949).

Kirn, F. S., Kennedy, R. J., and Wyckoff, H. O., Radiology, 63, 94 (July 1954).

Mood, A. M., Introduction to the Theory of Statistics, (McGraw Hill Publishing Company, Inc., New York, 1950).

Peebles, G. H., Phys. Rev. 83, 237 (1951).

Peebles, G. H., Gamma Ray Transmission Through Finite Slabs, (Rand Corporation report), report number K-240 (1952).

Perkins, J. F., J. Appl. Phys. 26, 1372 (1955).

Solon, Wilkins, Oppenheim, and Goldstein, Gamma-Transmission by RMS Angle Calculations, (USAEC Technical Information Service report), report number NYO-637 (1951).

Spencer, L. V., Phys. Rev. 88, 793 (1952).

Spencer, L. V., Penetration and Diffusion of X-rays by Semi-Asymptotic Methods, (National Bureau of Standards report), report number NBS-1726 (1952).

Spencer, L. V., and Fano, U., Phys. Rev. 81, 464 (1951).

Spencer, L. V., and Fano, U., NBS Jour. Res. 46, 446 (1951).

Spencer, L. V., and Jenkins, F., Part IV, Phys. Rev. 76, 1885 (1949).

Spencer, L. V., and Wolff, C., Phys. Rev. 90, 510 (1953).

Taussky, O., and Todd, J., Generation and Testing of Pseudo-Random Numbers, (National Bureau of Standards report), report number NBS-3370 (1954).

White, G. R., X-Ray Attenuation Coefficients from 10 Kev to 100 Mev, (National Bureau of Standards report), report number NBS-1003 (1952).

Wilkins, Oppenheim, and Solon, The Transport Equation in Straight-Ahead Case, (USAEC report), report number NYO-633 (1950).

Young, G., Piece-Wise Greuling Solution for Hydrogen, (Oak Ridge National Laboratory report), report number ORNL-415 (1949).

Young, G., On Straight-Ahead $\gamma$-Transmission with a Minimum in the Cross Section, (Oak Ridge National Laboratory report), report number ORNL-416 (1949).

# APPENDIX A

# APPENDIX A

This section describes the method used to determine the ratio of the response of an energy sensitive detector located on one side of an infinite slab where the radiation was incident over the opposite face to the response when the slab is removed. The ratio is termed the fraction of detector response in this paper. The detector was considered to be an infinitesimal sphere which has a response proportional to the energy of the incident photons. The response of such a detector, D, is given by

$$D = CA\Phi \tag{42}$$

where

$C$ = proportionality constant,

$A$ = cross sectional area of the detector,

$\Phi$ = energy flux (energy/unit area, unit time).

The expression for $\Phi$ outside the slab is

$$\Phi = \int_{\Omega} j(\theta,\phi)d \tag{43}$$

where

$j(\theta,\phi)$ = energy current per unit solid angle in a direction making the polar angle $\theta$ and azimuth angle $\phi$ with respect to the slab normal.

For the case of interest here, $j(\theta.\phi)$ is independent of position outside of the slab. Now let

$K(\theta',\phi')$ = the energy transmitted through the slab per unit surface area per unit time per unit solid angle in a direction making the polar angle $\theta'$ and azimuth angle $\phi'$ with respect to the slab normal.

Then the current on the side of the slab opposite the source face is

$$j(\theta',\phi') = K(\theta',\phi') \sec\theta', \tag{44}$$

and the detector response at the same point is

$$D_s = CA \int_{\theta'=0}^{\pi/2} K_1(\theta') \sec\theta' \sin\theta' d\theta' \tag{45}$$

where

$$K_1(\theta') = \int_{\phi'=0}^{2\pi} k(\theta',\phi') d\phi'. \tag{46}$$

If the incident radiation has an energy current $I_o$, then the response of the detector when the slab is removed will be

$$D_o = CAI_o. \tag{47}$$

The fraction of detector response is then

$$\frac{D_s}{D_o} = \int_{\theta'=0}^{\pi/2} \frac{K_1(\theta')}{I_o} \sec\theta' \sin\theta' d\theta'. \tag{48}$$

If the radiation is incident on the slab at an angle $\theta_o$, then the energy incident per unit area of slab surface per unit time is $I_o \cos\theta_o$. Thus the fraction of energy transmitted per unit angle $\theta'$ is

$$F(\theta') = \frac{K_1(\theta') \sin\theta'}{I_o \cos\theta_o}. \tag{49}$$

So (48) becomes

$$\frac{D_s}{D_o} = \int_{\theta'=0}^{\pi/2} \cos\theta_o \, F(\theta') \sec\theta' d\theta'. \tag{50}$$

Now $F(\theta')$ can be written as

$$F(\theta') = F_1(\theta')\delta(\theta' - \theta_o) + F_2(\theta') \tag{51}$$

where the first term on the right represents the part attributed to the uncollided photons and the second term that part attributed to the photons which have made at least one collision. Using the relation given in (51) for $F(\theta')$, (50) becomes

$$\frac{D_s}{D_o} = F_1(\theta_o) + \int_{\theta'=0}^{\pi/2} \cos\theta_o \, F_2(\theta') \sec\theta' d\theta' \tag{52}$$

where $F_1(\theta_o)$ is the fraction of energy transmitted through the slab by uncollided photons.

Table XIX gives a typical set of data obtained in the calculation. To obtain the fraction of energy transmitted in each of the angle intervals, the following equation was solved.

$$\overline{F_{2k}(\theta')} = \sum_m \frac{f_{km}}{\Delta\theta_k \, \alpha_m} \cdot \frac{(\alpha_m + \Delta\alpha_m)^2 - \alpha_m^2}{2} \tag{53}$$

where

$\overline{F_{2k}(\theta')}$ = the average value of $F_2(\theta')$ in the $k^{th}$ angle interval,

$f_{km}$ = fraction of photons transmitted in the $k^{th}$ angle interval and the $m^{th}$ energy interval,

TABLE XIX

ENERGY SPECTRUM OF PHOTONS PENETRATING A SLAB WITH DEGRADED ENERGY

Incident Photon Energy ($m_oc^2$): 2.45
Angle of Incidence (Deg): 0
Lead Thickness (cm): 2.5
Number of Sample Photons: 10,000

| Energy Range Units $m_oc^2$ | Fraction of Photons Transmitted | | | | |
|---|---|---|---|---|---|
| | 0-15° | 15-30° | 30-45° | 45-60° | 60-90° |
| 0.1727-0.2 | 0 | 0 | 0 | 0 | 0 |
| 0.2-0.3 | 0 | 0 | 0 | 0 | 0 |
| 0.3-0.4 | 0.0002 | 0 | 0 | 0.0001 | 0.0001 |
| 0.4-0.5 | 0.0003 | 0 | 0 | 0.0001 | 0.0001 |
| 0.5-0.6 | 0.0004 | 0 | 0 | 0.0001 | 0.0002 |
| 0.6-0.7 | 0.0011 | 0.0001 | 0.0003 | 0.0003 | 0 |
| 0.7-0.8 | 0.0011 | 0.0001 | 0.0004 | 0.0002 | 0.0002 |
| 0.8-0.9 | 0.0022 | 0.0002 | 0.0002 | 0.0005 | 0.0004 |
| 0.9-1.0 | 0.0038 | 0 | 0.0003 | 0.0005 | 0.0006 |
| 1.0-1.1 | 0.0040 | 0.0001 | 0.0005 | 0.0006 | 0.0004 |
| 1.1-1.2 | 0.0043 | 0 | 0.0007 | 0.0008 | 0.0026 |
| 1.2-1.3 | 0.0057 | 0.0001 | 0.0008 | 0.0006 | 0.0035 |
| 1.3-1.4 | 0.0063 | 0.0002 | 0.0004 | 0.0008 | 0.0047 |
| 1.4-1.5 | 0.0078 | 0.0003 | 0.0005 | 0.0045 | 0.0024 |
| 1.5-1.6 | 0.0092 | 0.0004 | 0.0009 | 0.0073 | 0.0006 |
| 1.6-1.7 | 0.0075 | 0.0004 | 0.0004 | 0.0064 | 0.0003 |
| 1.7-1.8 | 0.0086 | 0.0002 | 0.0006 | 0.0076 | 0.0002 |
| 1.8-1.9 | 0.0077 | 0.0006 | 0.0035 | 0.0036 | 0 |
| 1.9-2.0 | 0.0094 | 0.0005 | 0.0084 | 0.0005 | 0 |
| 2.0-2.1 | 0.0089 | 0.0003 | 0.0085 | 0.0001 | 0 |
| 2.1-2.2 | 0.0097 | 0.0003 | 0.0094 | 0 | 0 |
| 2.2-2.3 | 0.0111 | 0.0030 | 0.0081 | 0 | 0 |
| 2.3-2.4 | 0.0110 | 0.0109 | 0.0001 | 0 | 0 |
| 2.4-2.45 | 0.0049 | 0.0049 | 0 | 0 | 0 |

$\alpha_m$ = energy at the lower limit of the $m^{th}$ energy interval,

$\Delta\alpha_m$ = width of the $m^{th}$ energy interval,

$\Delta\theta_k$ = width of the $k^{th}$ angle interval.

The sum $\sum_k \overline{F_{2k}(\theta')}\Delta\theta_k$ for all cases calculated differed by less than 1 per cent from the value obtained during machine calculation by taking the average value of the fraction of energy transmitted by those sample photons having had at least one collision. The values of $\overline{F_{2k}(\theta')}$ for the case given in Table XIX are plotted in Fig. 15. A smooth curve was drawn through these average values giving an approximate curve for $F_2(\theta')$. Three requirements were made to fit the curve: (1) $F_2(0)$ is zero, (2) $F_2(\pi/2)$ is zero, and (3) the area under the curve in each angle interval (k) must equal the product $F_{2k}(\theta')\Delta\theta_k$. The curve for $\cos\theta_o\, F_2(\theta')\sec\theta'$ was then obtained using the approximate values from the curve for $F_2(\theta')$ and the integral performed as given in (52). The value for $F_1(\theta_o)$ was obtained from Table VI under the fraction of incident photons penetrating the slab without degradation in energy. The sum of the integral and $F_1(\theta_o)$ gives the fraction of detector response which was the value plotted in Fig. 9 at slab thickness 1.63 m. f. p.

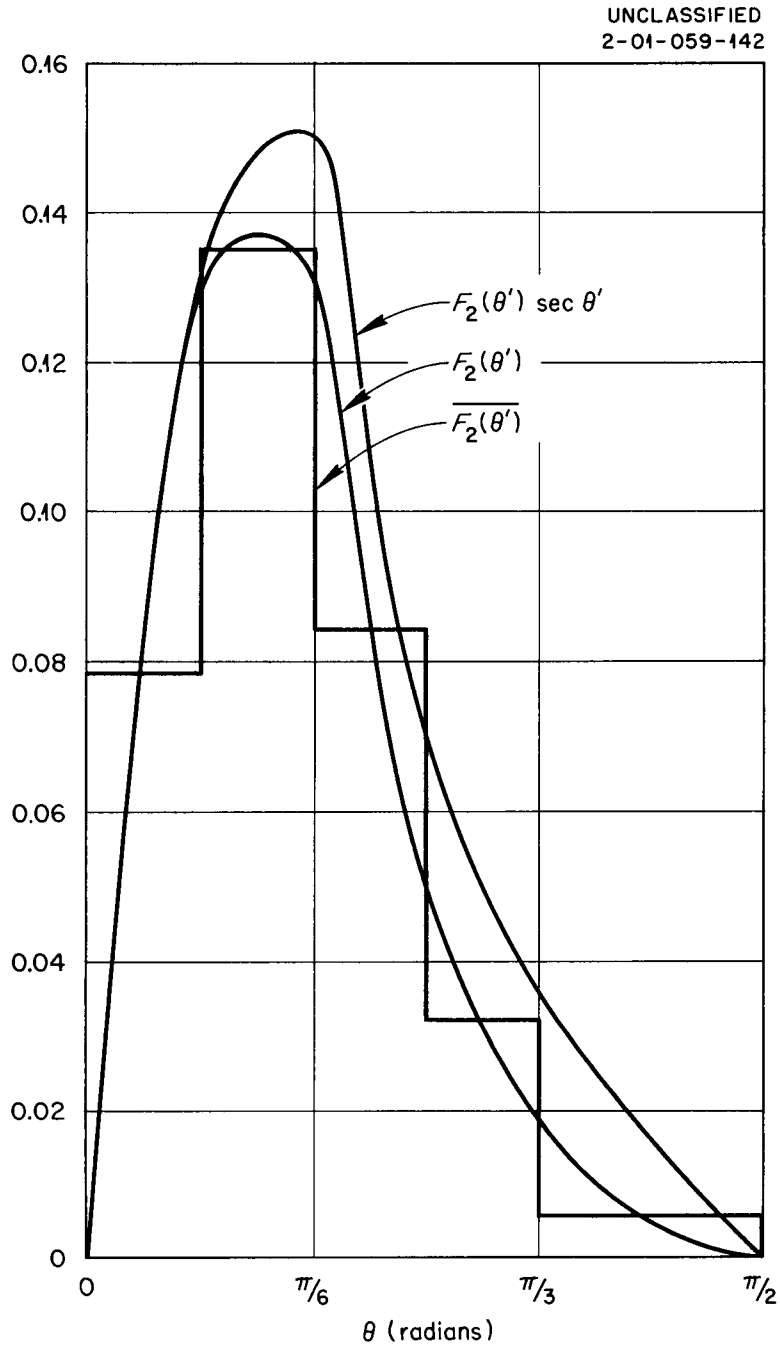


Fig. 15. Values of $\overline{F_2(\theta')}$, $F_2(\theta')$ and $F_2(\theta')$ sec $\theta'$ for the Case of 2.45-$m_0c^2$ Source Photons Incident at 0 deg on 2.5 cm of Lead.

# APPENDIX B

# APPENDIX B

The purpose of this appendix is to describe a method by which the fraction of energy transmitted through slabs for other than monodirectional monoenergetic sources can be obtained from the data presented. In what follows, all quantities are per unit surface area.

In general, the fraction of source energy penetrating a given slab is a continuous function which will be defined as

$G(\theta,\phi,\alpha;\theta',\phi',\alpha)d\Omega' d\alpha'$ = fraction of source energy $\alpha$ incident at angles $\theta$ and $\phi$ that penetrate the slab in the energy interval $\alpha$ to $\alpha + d\alpha$ and in solid angle $d\Omega'$ about the direction having angles $\theta'$ and $\phi'$.

The geometry showing the angles is given in Fig. 16. Because of symmetry, the function G can be rewritten as $G(\theta,\alpha;\theta',\phi'-\phi,\alpha')$. Let the distributed source be defined as

$S(\theta,\phi,\alpha)d\Omega d\alpha$ = source photons incident in solid angle $d\Omega$ about the direction having angles $\theta$ and $\phi$ and in the energy interval $\alpha$ to $\alpha + d\alpha$.

Now to obtain the fraction of energy penetrating the slab from the distributed source in any interval of the exit plane variables, the following equation must be solved:

$$P = \frac{\displaystyle\int_{\theta=0}^{\pi/2}\int_{\phi=0}^{2\pi}\int_{\alpha=0}^{\infty}\int_{\theta'=\theta''}^{\theta''+\Delta\theta''}\int_{\theta'=\phi''}^{\phi''+\Delta\phi''}\int_{\alpha'=\alpha''}^{\alpha''+\Delta\alpha''} \alpha S(\theta,\phi,\alpha)G(\theta,\alpha;\theta',\phi'-\phi,\alpha')d\Omega d\alpha d\Omega' d\alpha'}{\displaystyle\int_{\theta=0}^{\pi/2}\int_{\phi=0}^{2\pi}\int_{\alpha=0}^{\infty} \alpha S(\theta,\phi,\alpha)d\Omega d\alpha} \tag{54}$$

UNCLASSIFIED
2-01-059-143

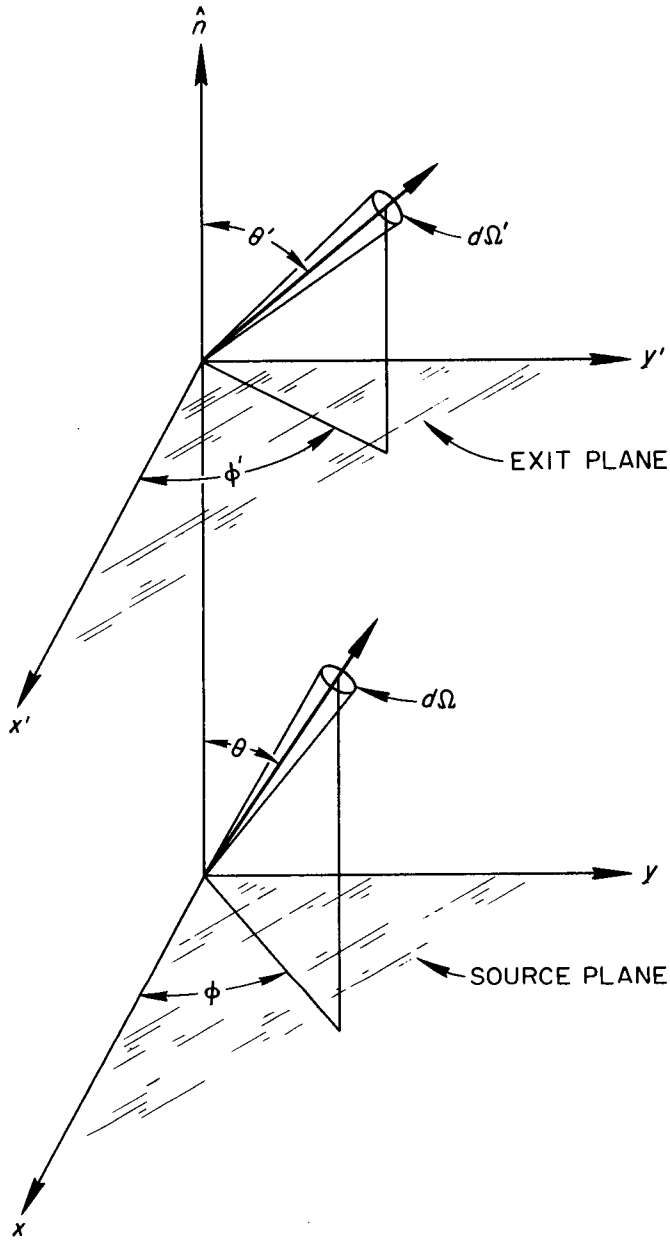


Fig. 16. Angle Variables for Source and Exit Planes of a Slab.

where $\theta''$ to $\theta'' + \theta''$, $\phi''$ to $\phi'' + \phi''$, and $\alpha''$ to $\alpha'' + \alpha''$ are the desired intervals of the exit plane variables.

Suppose, for example, it is desired to find the total fraction of energy penetrating a slab from a source defined as

$$S(\theta,\phi,\alpha) = L \cos\theta \, \delta(\alpha - \alpha_o) \tag{55}$$

where L is a constant. Substituting (55) into (54) and performing the integration gives

$$P_T = 2 \int_{\theta=0}^{\pi/2} \cos\theta \, G_1(\theta,\alpha_o) \sin\theta \, d\theta \tag{56}$$

where

$$G_1(\theta,\alpha) = \int_{\theta'=0}^{\pi/2} \int_{\phi'=0}^{2\pi} \int_{\alpha'=0}^{\infty} G(\theta,\alpha;\theta',\phi'-\phi,\alpha') \sin\theta' \, d\theta' d\phi' \, d\alpha' \tag{57}$$

As a practical example, suppose $\alpha_o$ is $6\text{-}m_oc^2$ and the slab was stratified with 9 in. of polyethylene followed by 0.3 in. of lead. The values of $G_1(\theta,\alpha_o)$ are given in Table XIII at values of $\theta$ of 0-, 30-, and 60-deg. Figure 17 gives a plot of $G_1(\theta,\alpha_o)$ as a smooth curve fit to the three data points. The extrapolation was made to $G_1(90^o,\alpha_o)$ equal to zero. Although this is not rigorously correct only a small error is introduced. Figure 18 gives a plot of $2uG_1(\mu,\alpha_o)$ where $\mu = \cos\theta$. This function was numerically integrated to obtain $P_T = 0.245$.

Other quantities for distributed sources can be obtained in a similar manner.

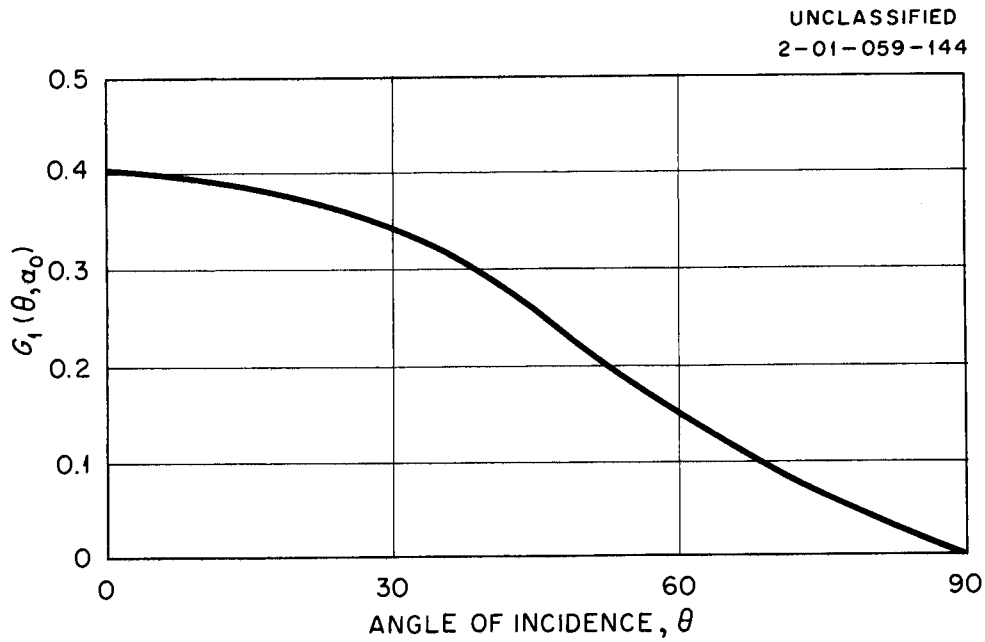


Fig. 17. Plot of $G_1(\theta, E_0)$ for Stratified Slab where 9 in. of Polyethylene is Followed by 0.3 in. of Lead and $\alpha_0 = 6\, m_0 c^2$.

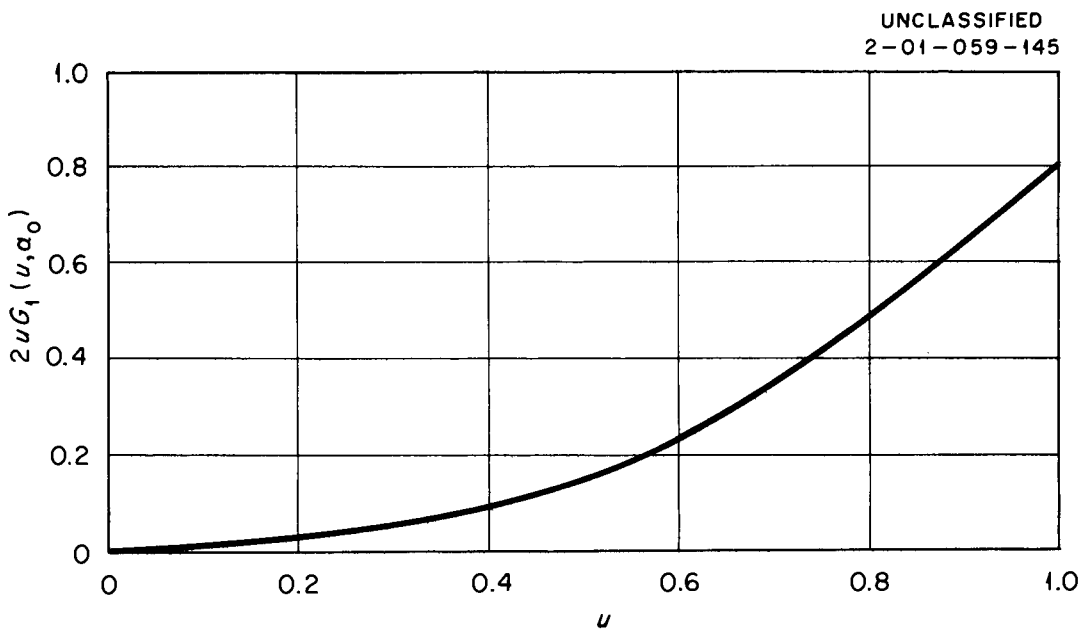


Fig. 18. Plot of $2uG_1(u, \alpha_0)$ for Stratified Slab where 9 in. of Polyethylene is Followed by 0.3 in. of Lead and $\alpha_0 = 6m_0c^2$.